NREL
NATIONAL RENEWABLE ENERGY LABORATORY

Cost and Reliability Improvement for CIGS-Based PV on Flexible Substrate

May 24, 2006 — July 31, 2010

Scott Wiedeman
Global Solar Energy
Tucson, Arizona

NREL is a national laboratory of the U.S. Department of Energy, Office of Energy Efficiency & Renewable Energy, operated by the Alliance for Sustainable Energy, LLC.

Subcontract Report
NREL/SR-5200-51604
May 2011

Contract No. DE-AC36-08GO28308

NREL
NATIONAL RENEWABLE ENERGY LABORATORY

Cost and Reliability Improvement for CIGS-Based PV on Flexible Substrate

May 24, 2006 — July 31, 2010

Scott Wiedeman
Global Solar Energy
Tucson, Arizona

NREL Technical Monitor: Harin S. Ullal
Prepared under Subcontract No. ZXL-6-44205-13

National Renewable Energy Laboratory
1617 Cole Boulevard
Golden, Colorado 80401
303-275-3000 • www.nrel.gov

Subcontract Report
NREL/SR-5200-51604
May 2011

Contract No. DE-AC36-08GO28308

Available electronically at http://www.osti.gov/bridge

Available for a processing fee to U.S. Department of Energy and its contractors, in paper, from:

U.S. Department of Energy
Office of Scientific and Technical Information

P.O. Box 62
Oak Ridge, TN 37831-0062
phone: 865.576.8401
fax: 865.576.5728
email: mailto:reports@adonis.osti.gov

Available for sale to the public, in paper, from:

U.S. Department of Commerce
National Technical Information Service
5285 Port Royal Road
Springfield, VA 22161
phone: 800.553.6847
fax: 703.605.6900
email: orders@ntis.fedworld.gov
online ordering: http://www.ntis.gov/help/ordermethods.aspx

Cover Photos: (left to right) PIX 16416, PIX 17423, PIX 16560, PIX 17613, PIX 17436, PIX 17721

Printed on paper containing at least 50% wastepaper, including 10% post consumer waste.

Table of Contents

Executive Summary

When this TFPPP subcontract was partially completed, Global Solar Energy (GSE) was charged with simultaneously executing a dramatic increase in production capacity, with the planning and construction of two entirely new production facilities for thin film CIGS PV (in Tucson, AZ and Berlin, Germany). The expansion was the major focus of the organization for about 24 months, and in some cases diverted resources that had been allocated to development, including this subcontract. However, since the expansion required entirely new production equipment for all phases of the thin film deposition and "back-end" operations, it also provided a unique opportunity to execute on the goals of this subcontract in ways we had not envisioned. Major improvements in cost and reliability, goals of this subcontract, could now be addressed in the design stages for the 'Gen2' plants and equipment, opening up large opportunities, and leveraging what had been learned at GSE with the existing 'Gen1' production equipment and processes.

The expansion entailed the selection, negotiation and purchase of a 120,000 sq. ft. facility on 22 acres in Tucson, and planning for another complete factory in a leased facility in Berlin. Extensive architectural and design work allowed efficient, balanced production in all processes, in a fully facilitated, climate-controlled, state-of-the-art thin film manufacturing plant. Simultaneously, lines of entirely new production tools for all processes were taken from concept, through design, vendor selection and into fabrication and installation for both plants. Previous experience gained by GSE in bringing the world's 1st generation of roll-to-roll CIGS processing equipment to 4 MWp/year production was fully leveraged in the design of the 2nd generation tools for the new plants in Tucson and Berlin. The 2nd generation thin film production tools are designed to run faster, longer, better and with greater process complexity, reproducibility, higher materials utilization, and less labor and maintenance cost.

While the scale of the plant expansion is rapid, the new production tools represent an evolutionary progression of the Global Solar CIGS technology. Manufacturing cost has been reduced by increased automation, higher materials utilization, and greater capacity with higher rates in all tools. These advancements garner reduced capital expense, a smaller factory floor area requirement, and greater productivity in addition to reduced direct product cost. Product reliability and product design for durability has also been a successful focus of this effort. Significant process optimization at the higher production rates of the "Gen2" equipment and cost reduction as embodied in the goals of this subcontract have been accomplished during this TFPPP subcontract.

Introduction of thin film PV into the solar market place has accelerated dramatically in the past year, delivering on the promise of performance, stability and low cost, which in turn were promoted by advances in efficiency, manufacturing cost reduction, and by design improvements for stability. Significant potential for further improvement in the factors driving thin film PV into the commercial market is enabled by several key concepts which were first initiated by Global Solar Energy (GSE). The key concepts pioneered by GSE include roll-to-roll deposition, thin stainless steel foil substrate, in-situ real time process monitoring for intelligent control, and highly automated backend assembly using $CuIn_xGa_{(1-x)}Se_2$ (CIGS)[1,2]. The selection of CIGS enables very high ultimate efficiency, using very thin layers of a semiconductor that is fundamentally stable. Steel foil substrate enables low cost and low materials usage in high

temperature processes with rapid thermal equilibration times, and roll-to-roll processes with flexible product. Roll-to-roll methods allow continuous production with real-time control in very compact, low cost deposition equipment, minimizing capital expenditure and required factory size. Real-time, in-situ sensors with intelligent process control enable high manufacturing yields at rapid rates. Both rigid and flexible end products, addressing multiple markets, can be made by starting with flexible substrate. Successful implementation of these key concepts, with economies of scale, maximize commercial potential.

Continued testing of module reliability in rigid product has reaffirmed extended life expectancy for standard glass product, and has qualified additional lower-cost methods and materials. Expected lifetime for PV in flexible packages continues to increase as failure mechanisms are elucidated, and resolved by better methods and materials. Significant cost reduction has been enabled in the front contact process through designs having better materials utilization, and in the back contact process through enhanced vendor and material qualification and selection. The largest cost gains have come as a result of higher cell conversion efficiency, higher processing rates, greater automation and improved control in all process steps. These improvements are integral to this TFPPP program, and all realized with the 'Gen2' plants, processes and equipment.

Dramatic increases in module efficiency, which can now exceed 13%, are evident at GSE factories in two countries with a combined capacity greater than 75 MW. During 2009 the average efficiency of cell strings (3780 cm^2) was increased from 7% to over 11%, with "best" results exceeding 13% (Fig. s1). These results reflect all the cell production in the Tucson plant on the Gen2 equipment (commissioned in 2008) for all steps.

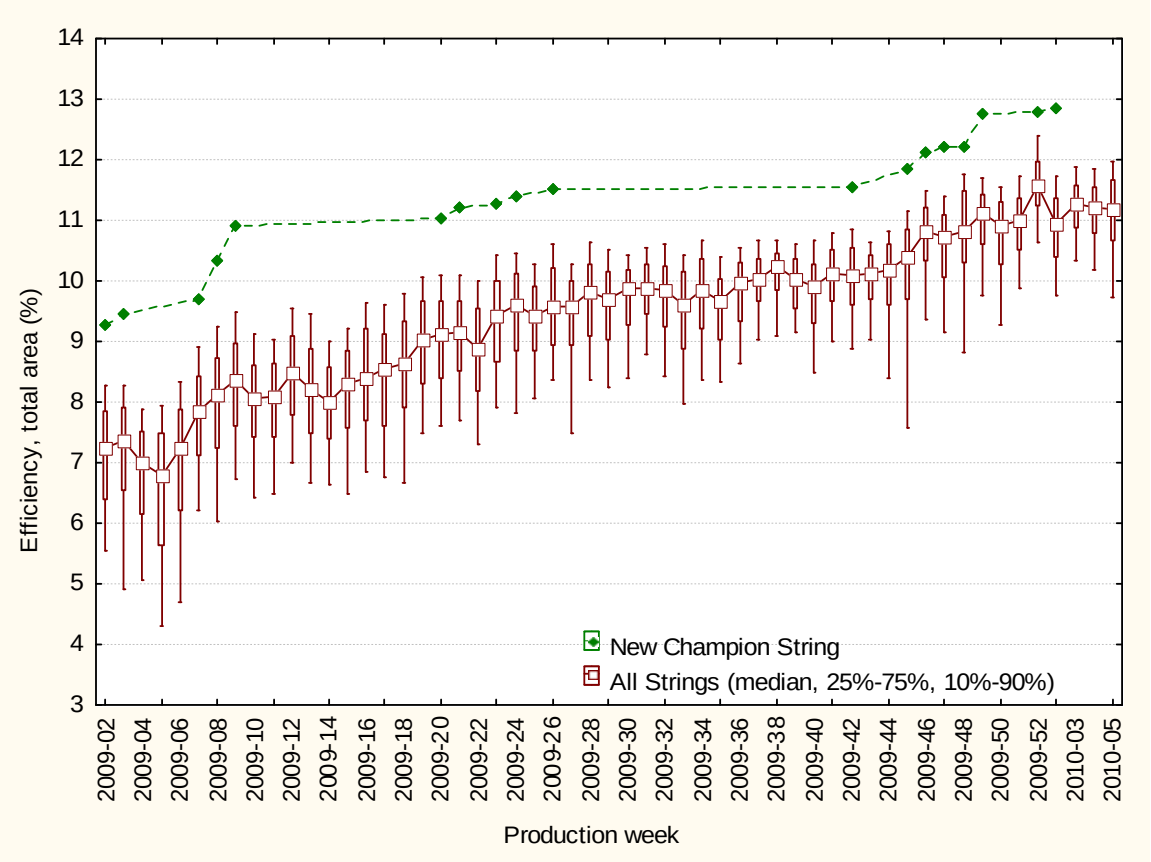

Fig. s1. Efficiency vs. time of full "strings" from the manufacturing line at GSE, showing all results and best results over the course of the factory ramp-up.

The "Gen2" design is substantially larger (210x100 mm) than earlier Gen1 product. The Gen2 design also entailed a different interconnect method, using tabbing and stringing equipment similar to that used commonly for crystalline silicon PV. The basic product, shown in Fig. s2a, is intended for applicability to several markets, including rigid product and "Building-Integrated" (BIPV) applications. Standard format rigid GSE panels using the Gen2 cells have been certified by NREL at over 190 W at standard conditions. These cells from GSE have been used in rigid product to erect the largest CIGS rooftop installation in the world, comprising 820 kWp of CIGS PV on 7+ acres of roof space, in Vincenza, Italy (see figure s2b). The earlier Gen1 cells continue to operate successfully in large power fields, as shown in figure s3 for the 750 kW_p field in Tucson, AZ.

Fig. s2a,b. A "Gen2" cell at GSE (210 cm^2), and modules made with Gen2 cells at the largest rooftop CIGS installation in the world (820 kWp at Vincenza, Italy). (Credit: Global Solar Energy)

Fig. s3. The GSE factory in Tucson, showing the ground-mounted 750 kWp CIGS power field in AZ. (Credit: Global Solar Energy)

Product reliability continues to evaluate favorably even for 'Gen1' product, operating with excellent field reliability on glass-encapsulated CIGS products. In particular, a 750 kW PV system on the grounds of the GSE Tucson facility was commissioned in late 2008 (fig. s3), and has been consistently producing at higher than rated expectation.

Actual product cost is intimately linked to production yields and thus have also been a major focus of effort. Production yield at both factories, shown in figure s4, has similarly progressed and now can exceed 95% in electrical test. The rapid advance shown in yield relate to progress in control, reproducibility and process development during this subcontract. In this respect reliance on in-situ monitoring for real-time intelligent process control, and operator training is crucial for reproducibility. The data also demonstrate the successful bi-directional transfer of necessary technology and information between GSE factories operating at differing locations, so that the same processes and equipment produce essentially the same results despite the complexity involved.

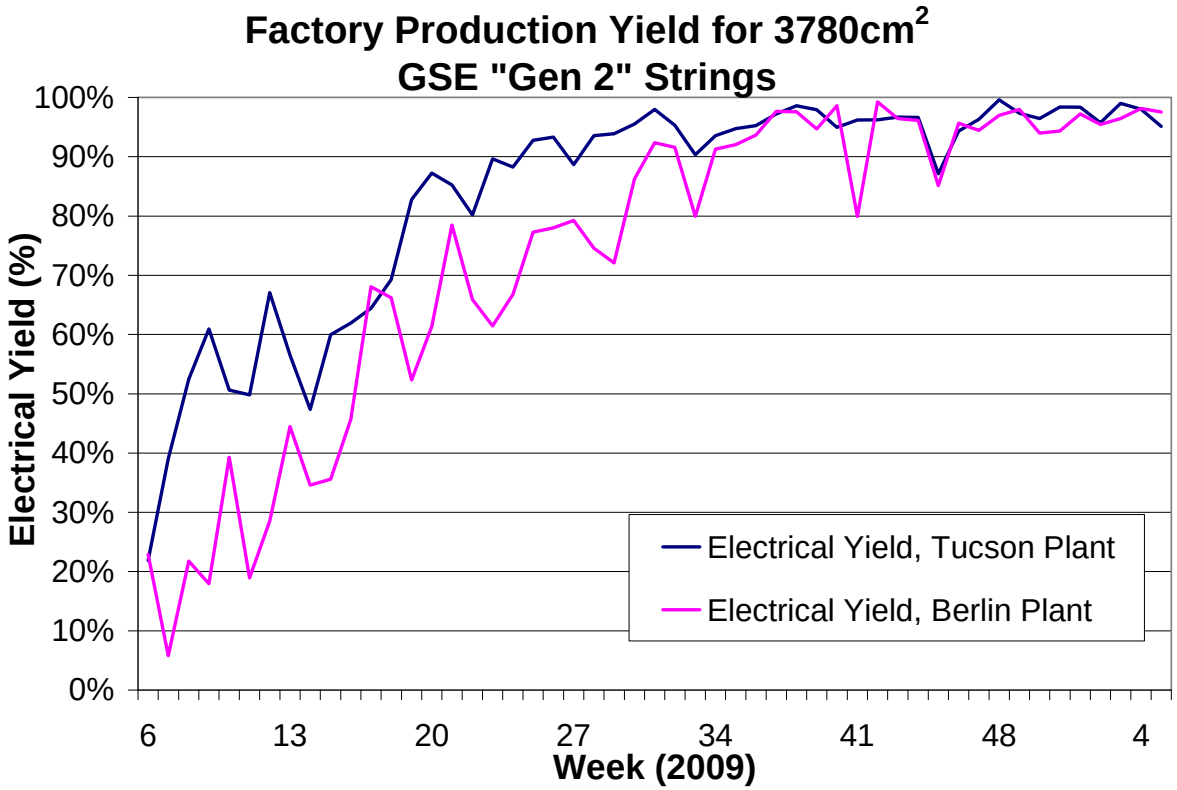

Fig. s4. Production yields for GSE "Gen 2" strings in 2009, at both factories. Electrical yield is the fraction of all strings that pass electrical performance tests (> 8% Efficiency).

Another representation of the progress made in overall efficiency, concurrent with gains in control and reproducibility that translate to improved yield is shown in figure s5.

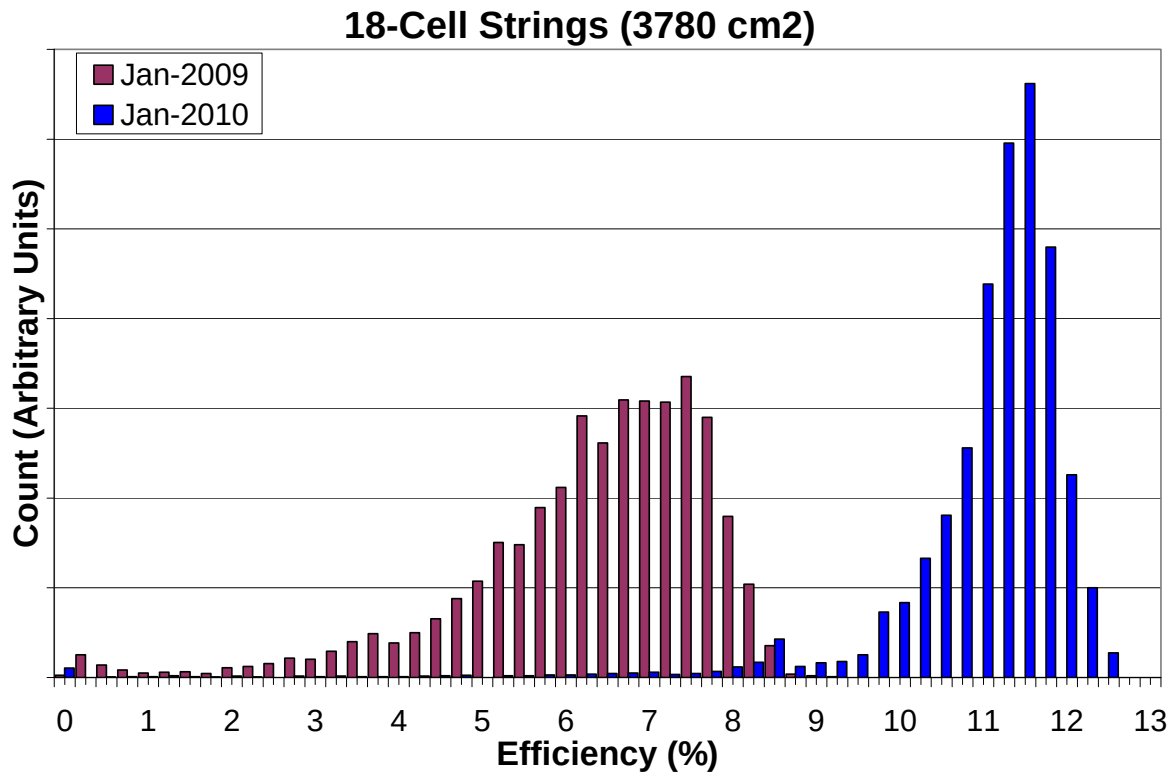

Fig. s5. A histogram of string (210 cm^2 cells x 18 cells each) production from the start of 2008 compared with 2009 from the GSE factory in Tucson.

The shift in "string" efficiency to a higher average, concurrent with a more desirable distribution is evident, reflecting improvements in multiple processes at GSE during 2009.

Figure s6 shows a champion module made using standard production processes and cells. This 3880 cm^2 module was measured by NREL, producing over 50 Watts at 13.2% aperture area efficiency, and was made using a string of 18 cells (210 cm^2 each). The cells were not specially selected or matched, but resulted from standard manufacturing processes and equipment at GSE.

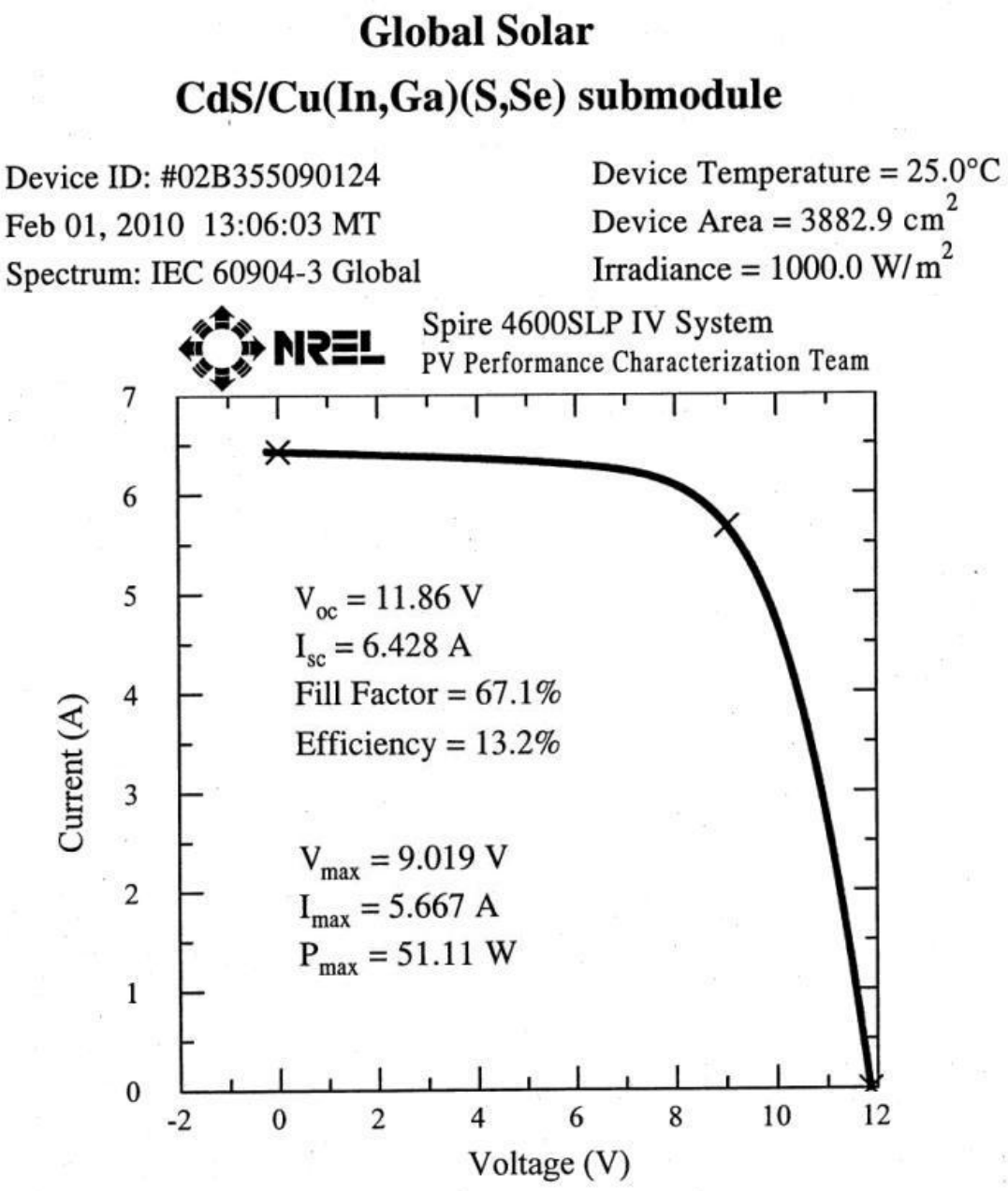

Fig. s6. An NREL measurement of a module made at GSE from a string using all standard, production processes and equipment (51.1 Watts, 13.2% efficiency, 3883 cm^2 area).

Beyond further improvements in reproducibility and control, there are significant power losses present in the current cell and interconnection design. Figure s7 shows the IV characteristic of a 15.4% small area device using standard GSE production CIGS on the flexible foil substrate, but finished using front contacting layers and grid made at NREL. Analysis of the results affirms that a significant increase in efficiency is available through improvement in the current collection and cell interconnection components.

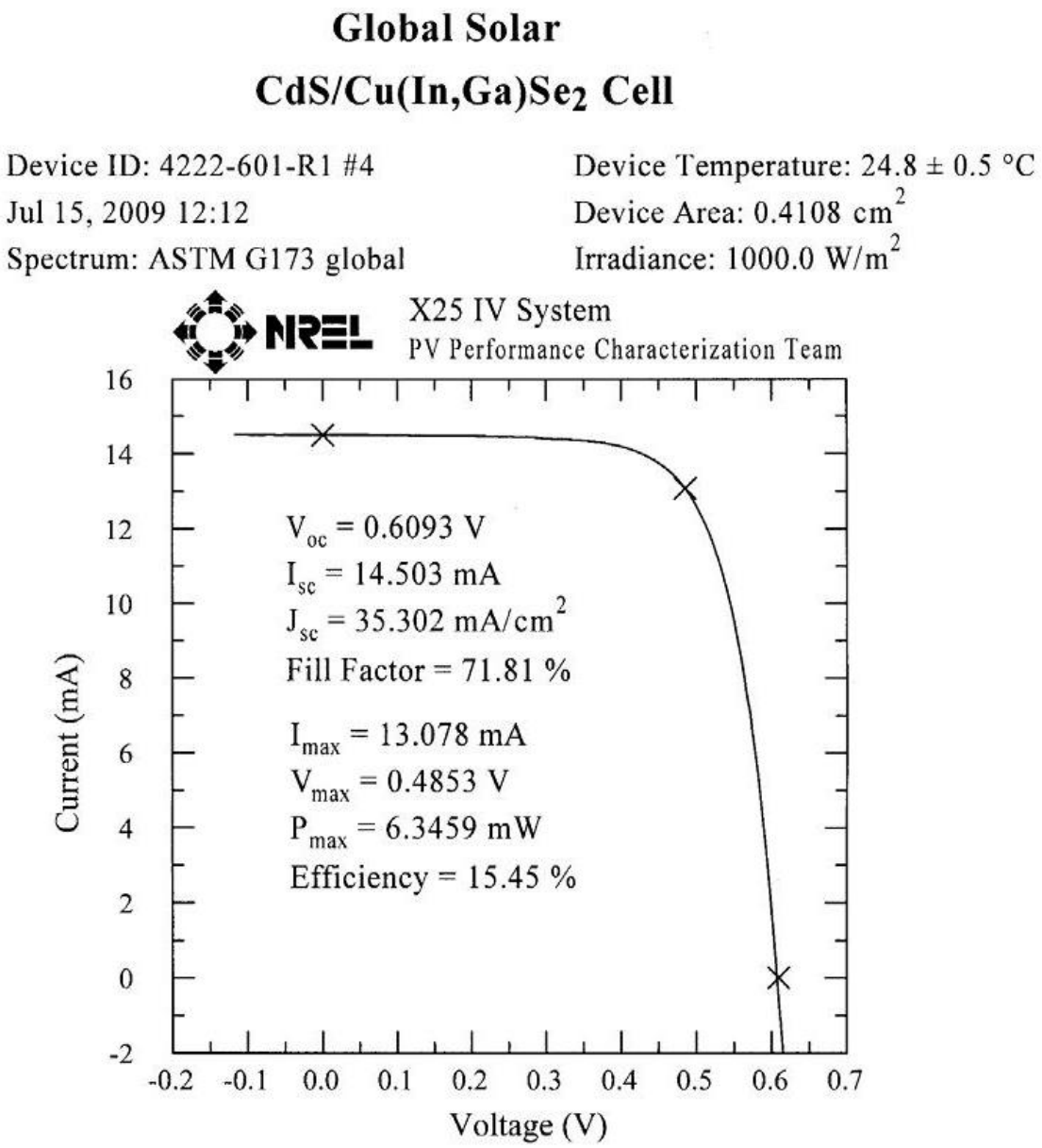

Fig. s7. The IV characteristic of a 15.4% efficient small area device made with GSE production material using a grid and contacting layers made at NREL.

Acknowledgements

We gratefully acknowledge support from NREL under subcontract ZXL-6-44205-13 and valuable discussion, measurements and technical guidance by Drs. Harin Ullal, Ingrid Repins, Rommel Noufi, Steve Rummel, and Keith Emery. We also acknowledge assistance from HZB Berlin under a joint work package with GSE. We would also acknowledge all the GSE employees and contractors, both in the U.S. and in Germany, who worked together to make these GSE advancements possible.

List of Figures

List of Tables

Task 1: Enhanced Module Reliability (Objectives)

1. Identify, characterize and quantify degradation and failure mechanisms in the PV stack and cell interconnect as well as encapsulation structure and complete module package.
2. Design meaningful stress tests for flexible and rigid thin film CIGS modules.
3. Develop a finite element model predicting mechanical post-lamination stresses at module operating conditions (daily and seasonal temperature cycles).
4. Explore solutions to eliminate failure & degradation mechanisms via process changes, advanced alternate encapsulation, protective coatings, structural elements and complete package.
5. Verify and optimize long-term product reliability.
6. Improve product appearance and cost.

Product Types and Testing

The specific tests required depend on the product type. For GSE, product is separated into three broad categories: portable flexible product, rigid PV for power use, and flexible power product for power or BIPV use. Portable flex product is intended for intermittent use where features of durability, portability and appearance are valued over long term reliability. Rigid PV products are intended for rooftop and commercial bulk power generation where power density and long term reliability (20 – 30 years) are crucial. Flexible power product has all the requirements of rigid PV products, but has added requirements for flexibility, weight and appearance.

Both real-time and accelerated testing is important to determining reliability, durability, failure modes and their causes. Specific to the product type above, GSE uses multiple methods to evaluate suitability, including actual outdoor exposure testing, accelerated testing in dedicated chambers or heightened stresses, and standardized tests.

Portable Flex Product

A battery of tests is shown below, which was devised in this example to pre-qualify flexible product for UL testing.

Table 1.1 - Pre-UL testing – a battery of tests run at GSE representing many of the procedures included in UL testing for 6 and 12 watt flex product.

Bonding Path resistance
Leakage Current
Dielectric Voltage Withstand
Water Spray
Leakage Current
Dielectric Voltage Withstand
Pull Test
Push Test
Wet Insulation Test
Dielectric Voltage Withstand

After continued improvement of procedures and materials used in product assembly, GSE portable product tested using the sequence above passed all tests.

As a typical example of iterative product reliability improvement, a failure mode due to lengthy cycles of folding and unfolding was noted for portable flex product, traced to the conductors used for internal circuitry, determined to be metal wire fatigue and separation. An alternative wiring scheme for the portable folding product was proposed and evaluated. Accelerated tests were made with equipment set up to continuously fold and unfold the product and monitor for failure in the fold zone. The alternative wiring scheme showed a 5x increase in the MTBF, which was sufficient for the expected product lifecycle. The alternative scheme was implemented for all product anticipated to require significant flexing in typical use.

Outdoor testing of flex modules for long term exposure under actual outdoor conditions has also been valuable in relative comparisons of product variations, and in identifying modes of failure. When a new failure mode is identified, specific tests are usually designed to isolate that failure mode under controlled conditions using quantitative means. Experience gained in identifying failure modes in outdoor testing and in accelerated testing has allowed GSE to establish protocols for test article submission for both modules and submodules of flexible and glass based products.

Rigid PV Product

This product has a structure generally using glass / PV / backsheet, where the backsheet can be glass or a combination of polymer and metal foil. Early field observations in identified some delamination in glass product under outdoor tests. “Pull tests” were incorporated into standardized testing at GSE to gauge adhesion strength as a function of the laminating materials, procedures and product exposure history. For example, the adhesion strength of several laminating materials to glass was tested versus several different cleaning methods. A method of chemically priming the current laminating materials was evaluated using the same standardized adhesion “pull test”. In this case pull tests indicated consistently higher adhesion without using

this priming compound. Although other factors are considered (material availability, process speed, reproducibility, etc.), generally the best settings and materials as indicated by the standardized test are selected for further testing, including outdoor tests.

Standard tests for electrical performance measures have also been devised. Curing profiles and multiple types of electrically conductive inks were iteratively tested to improve the resistance of printed cell grid patterns. Process settings can have dramatic impact; one test demonstrated an adjusted curing profile that resulted in a printed pattern resistance 55% lower than the "standard" curing profile.

Reliable stringing methods, using compatible materials are required to avoid interconnection failures. Again, failure modes were identified, and experiments to evaluate stress effects were completed, resulting in a preliminary selection of compatible stringing materials for glass product.

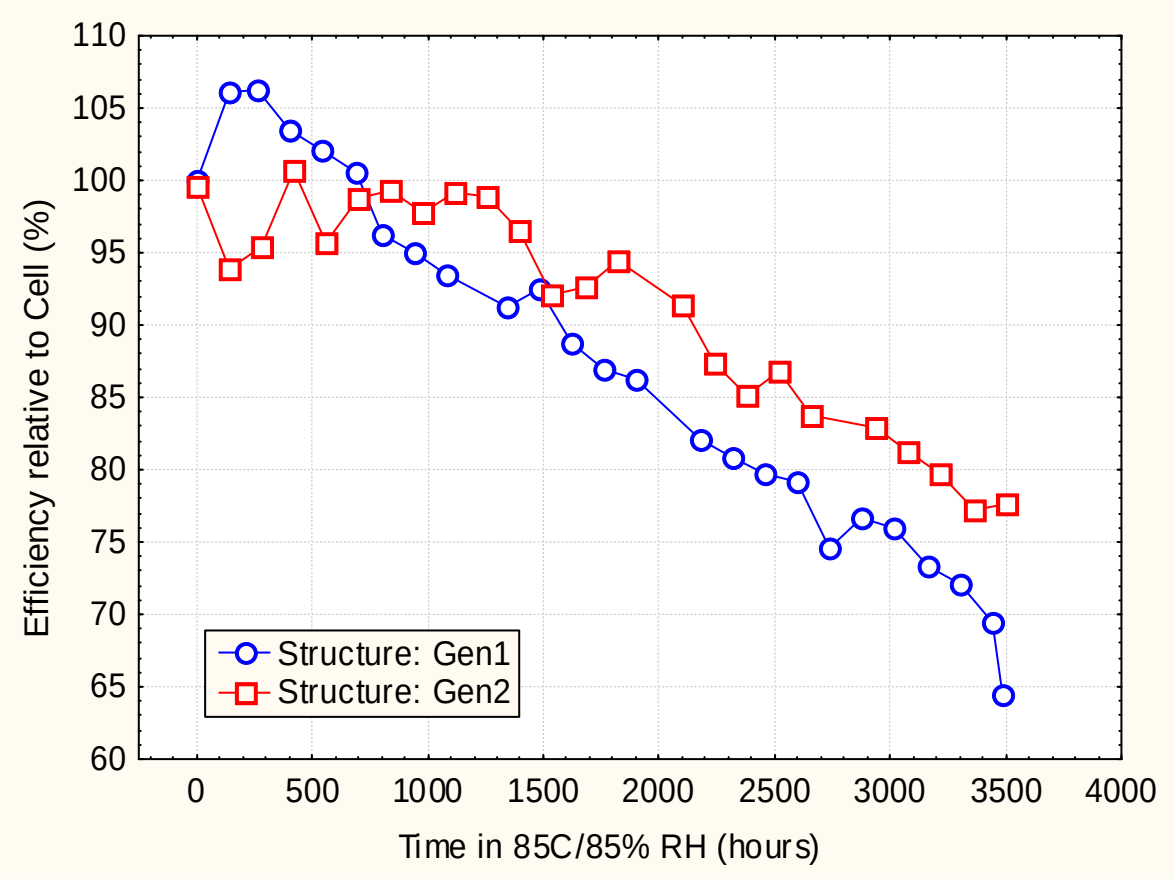

Fig. 1.1. A comparison of glass module performance in damp heat (85°C, 85% Relative Humidity) using first and second-generation string technologies with identical packaging. The modules (15 and 10 in each group, respectively) were light-soaked between 4 and 10 hours prior to each measurement.

Naturally, changes in construction materials or processes used for module fabrication invariably demand reliability testing, so reliability tests were initiated for strings of cells fabricated using a new TCO process for instance, to confirm the absence of ill effects.

Moving to 'Gen2' from 'Gen1' cell size and fabrication lines for the expanded GSE production required thorough testing for performance and reliability. Gen2 cell strings were fabricated by a manual technique to define the specifications for an automated stringing tool. Materials were down-selected for string connection based on conductivity, mechanical stress, and capability of application in high speed equipment. The new generation strings (laminated into glass modules) demonstrated satisfactory performance under accelerated testing (Figure 1.1).

Generally, cells or modules made with the standard process and materials are used as "controls" for comparison to results from the "new" process or method using accelerated testing (usually 85/85 damp heat testing). Other examples of the rigor required for process changes include the tests done for new materials for electrically connecting cells, which were procured and evaluated against the standard material for adhesion and module performance, before and after stress testing.

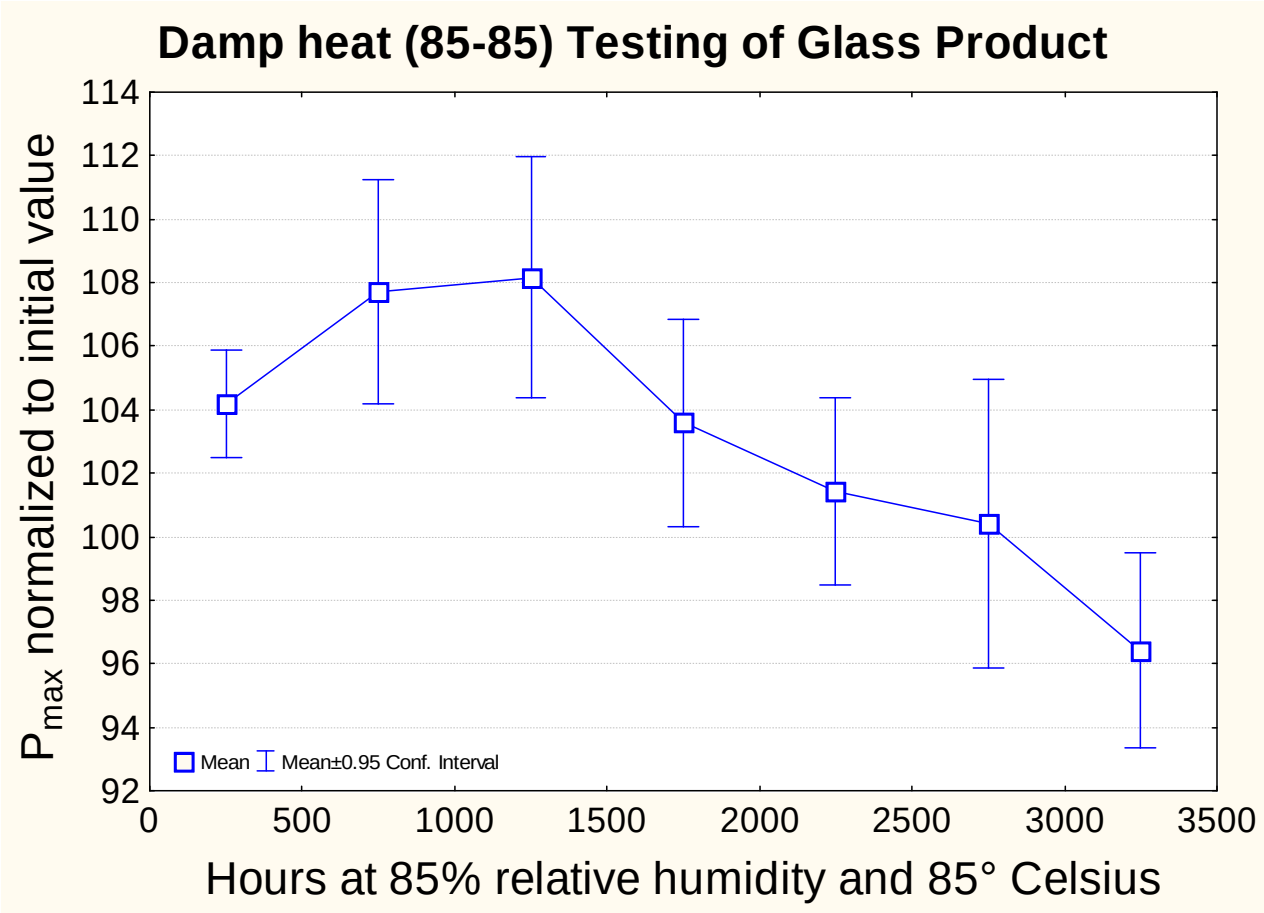

Fig. 1.2. An example of accelerated testing in progress at GSE. One combination of materials and assembly procedures is tested in damp heat (85°C, 85% relative humidity) for extended time. Normalized power output greater than 100% are often observed due to "light soak" effects typical of CIGS PV.

The "Damp Heat" test at 85°C and 85% relative humidity is typically one of the most demanding tests for module reliability, thus it is used frequently to gauge progress in reliability. Iterative testing of alternative materials and assembly techniques has improved the expected reliability of glass-based product. GSE has been able to demonstrate results that bode well in this regard (one example shown below in Fig. 1.2 for glass product).

While testing of different product configurations and laminates continues in the damp heat (85°C, 85% relative humidity) to build accelerated test data, glass-based product also continues in outdoor test deployment to gather performance data under actual conditions. Ultimately the data gathered using accelerated and real-time testing will allow the validation of models relating accelerated test data and life expectancy under actual conditions of use.

The rigid product that has shown reliability in accelerated tests continues to show stable operation under actual outdoor use. Early glass-based product, deployed at Springerville, AZ for long-term outdoor testing functioned with little degradation over several years (Fig 1.3). The performance over increasing time has shown substantially stable behavior, although recent more data is unavailable due to the failure of a large transformer connecting the inverter to the grid.

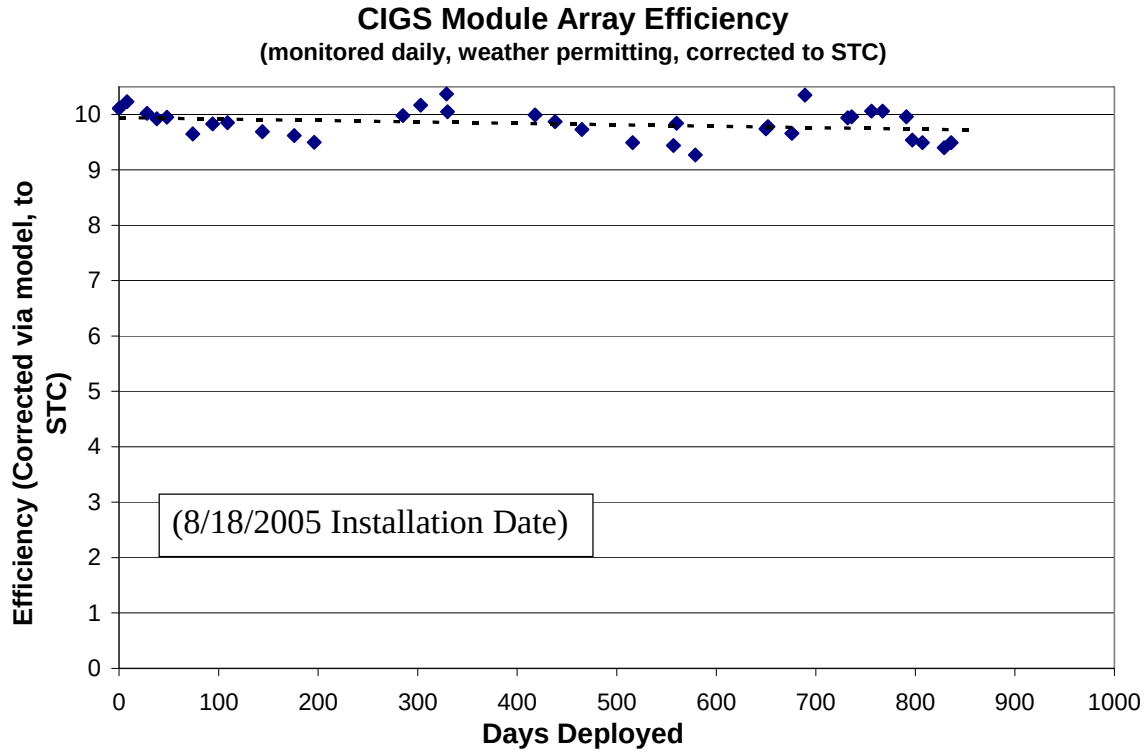

Fig.1.3. Performance data taken over an extended time for GSE glass-based product in actual outdoor use. These modules are early versions of glass-based product, and thus did not incorporate many of the improvements developed under this program.

The edges of the module potentially introduce unique failure mechanisms for glass-based PV due to moisture and O_2 ingress. Methods and materials for "edge seals" have been developed to counter this effect. The impact of one such edge sealing method on strings laminated in glass/backsheet modules is shown in Fig. 1.4. Edge seals were applied to six test modules, and six additional test modules that were otherwise identical were used as controls. Modules were qualified by light-soaking outdoors for three days followed by pulsed-light measurement after stress in damp heat for those under test. After almost 2000 hours in damp heat, the samples with edge sealant were on average unchanged in power from their starting power, while that of the controls (without edge seals) degraded to approximately 94% of the starting power. The difference between the two sets was statistically significant with 90% confidence. The two sets primarily differed in open-circuit voltage. The results indicate that the impact of edges and seals on the product must be considered.

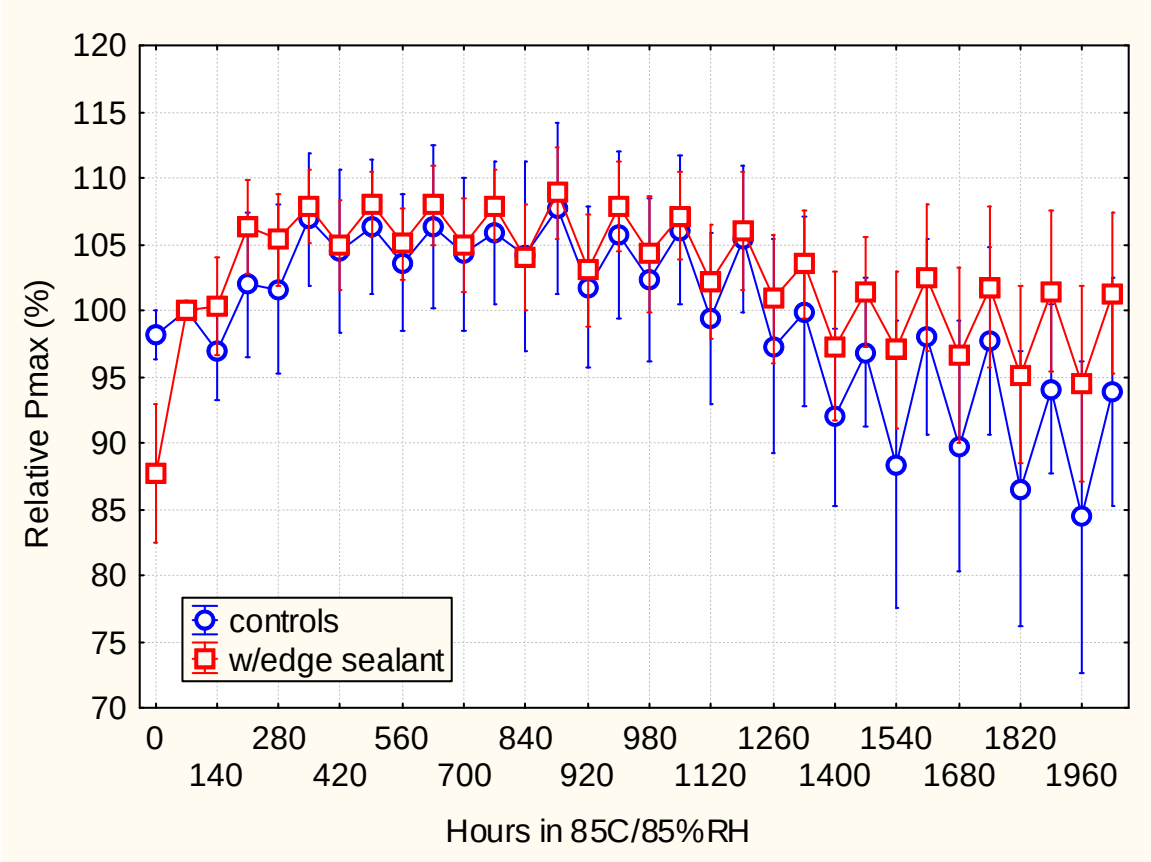

Fig.1.4. The mean relative power output of 2 groups modules (with and without edge sealant) vs. exposure time in damp heat (85/85). The regular point-point, low-high variation during the measurement is due to sequential measurement before, and then after light soaking upon each removal from the damp-heat exposure.

Possible interactions with corrosion mechanisms as a mode of degradation and voltage bias have also been studied at GSE. Normally, modules stressed in damp heat (85°C/85%RH) are maintained in the dark under open-circuit conditions. A test was run in which groups of modules were subjected to either damp heat under forward bias or under open circuit bias. Another goal of the test was to determine whether continuous forward-bias during accelerated testing had an effect on light-soaking characteristics.

Initially no clear difference in response due to bias in the dark under accelerated (85/85) conditions was seen, but at times approaching 2000 hours a difference emerged (Fig. 1.5). Modules that were forward-biased during damp heat stress were found to deteriorate more slowly than un-biased modules, to a statistical confidence level greater than 99%.

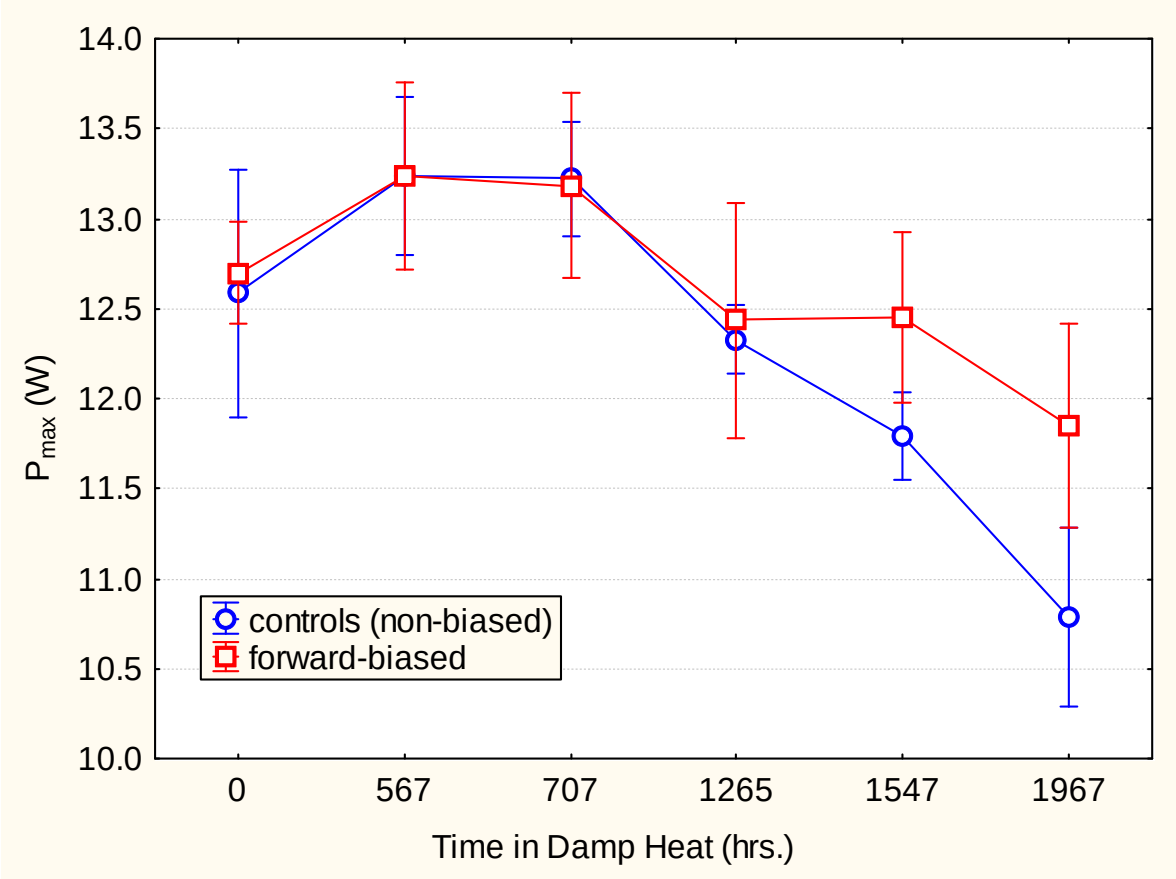

Fig. 1.5. Mean P_{max} of modules packaged in glass/backsheet; forward-biased near V_{max} and controls (non-biased) in damp heat testing in the dark.

Since electrochemical corrosion mechanisms are driven by differences in potential, failure mechanisms may also be different in light as compared to dark conditions. Other studies were conducted at GSE to determine the impact of corrosion under illuminated conditions using accelerated tests.

Twelve glass modules were fabricated and randomly assigned to two groups. Modules in one group were maintained at their individual Vmax (under AM1.5 illumination) during damp heat (85/85) treatment. Modules in the second group were not voltage-biased. After 560 hours of treatment, no statistical difference was observed between the two groups (Fig. 1.6). However, the two groups differed in their response to light-soaking following each treatment interval. Modules maintained at forward bias declined in Pmax by 1-4% upon lightsoaking. Modules not biased generally increased in Pmax upon lightsoaking, and the magnitude of improvement increased with increasing treatment time. In any case, no difference in light-soaked performance under standard conditions was noted in the two groups held at different voltage biases under illumination in this accelerated test.

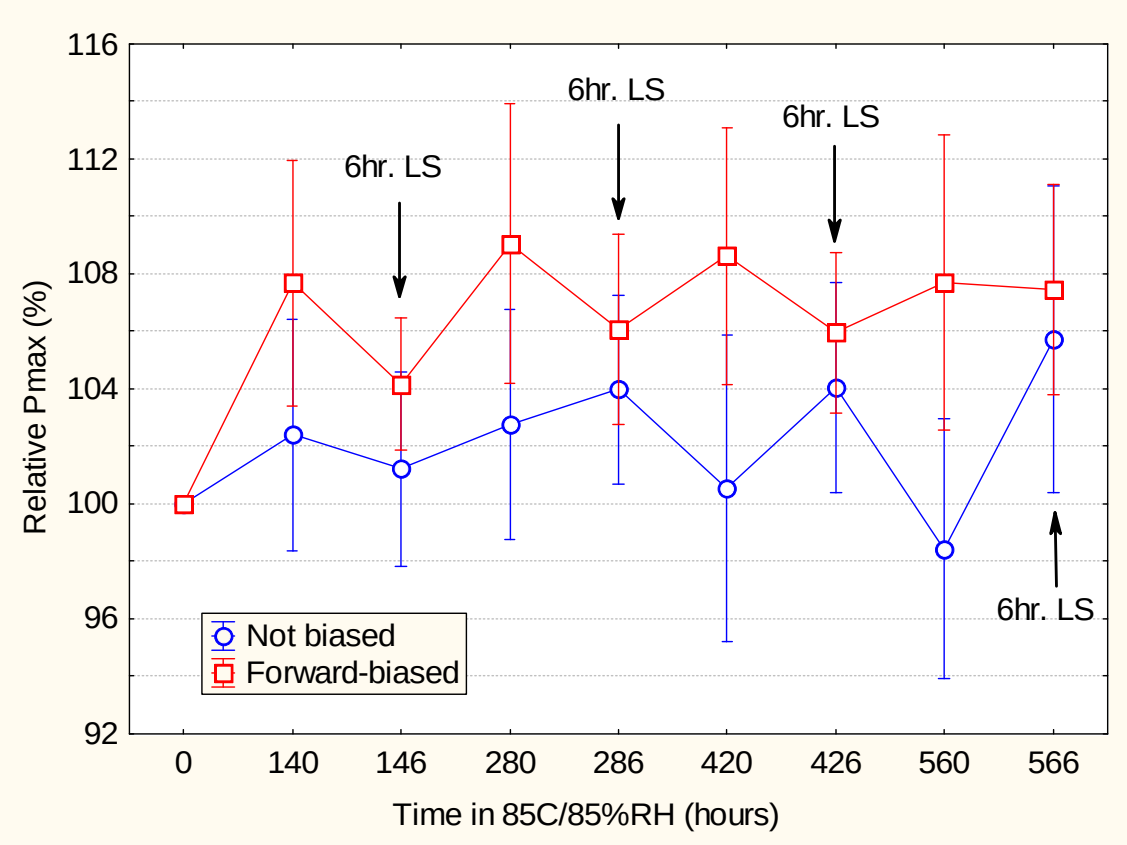

Fig. 1.6. Mean relative Pmax of CIGS strings laminated in glass, non-biased and biased at V_{max}, during damp heat treatment.

By nature, PV product requires many cell interconnections, each of which represents a potential point of failure. Accordingly, special test structures were developed to evaluate the reliability of the cell interconnects within strings or modules. The focus of this evaluation was finding changes in series resistance when exposed to thermal cycling and damp heat. The variable results that were obtained clearly indicated that a better understanding was required. At length, further investigations indicated that several modes of failure were involved, including electrochemical corrosion between dissimilar surfaces, simple mechanical failure due to differential thermal expansion, and other mechanisms. The reliability and failure mode was highly dependent on the materials and construction methods. Despite the complexity, and an understanding that is still incomplete, workable solutions appear to have been identified which indicate relatively stable series resistance in a glass package when subjected to damp heat, thermal cycling and humidity-freeze tests.

In preparation for IEC certification, glass-backsheet modules constructed from production strings were evaluated in damp heat tests (85°C/85% Relative Humidity) at GSE. Thermal cycling and humidity-freeze tests were conducted by a subcontractor. IEC 1646 protocol was used with an exception to the IEC standards in the thermal cycling test (only 155 cycles were conducted, not 200 cycles as specified in IEC 1646). Results are summarized below.

Using two 18-cell strings in each module, six modules were submitted for humidity-freeze tests, and five identical modules for thermal cycling. Since the GSE damp heat chambers are unable to

accommodate modules fabricated from 18-cell strings due to size, 12 modules were manually fabricated with 12 cells each in a 4x3 configuration (cut from 18-cell strings) for damp heat testing. The initial efficiencies of all tested modules were 9-10%.

Prior to initial and final measurements light soaking was conducted for 3-4 sunny days in Tucson (March 2009). The mean results, summarized in Table 1.2, indicate no significant losses after thermal cycling and humidity-freeze stress tests. A 10% loss in P_{max} after damp heat testing was observed, primarily due to fill factor loss. Steps required for the manual reconfiguration of the modules for damp heat testing may have been responsible for a portion of the loss observed in the damp heat test, as other damp heat tests on similar product has shown less power loss over longer exposure times.

Table 1.2.- Module performance changes after stress testing.

	Relative % Change upon Accelerated Stress		
Parameter	**DH-1000**	**TC-155**	**HF-10**
V_{max}	-7.6	3.9	1.7
I_{max}	-2.4	-1.1	-1.0
P_{max}	-10.0	2.6	0.4
V_{oc}	-0.7	1.5	1.1
I_{sc}	0.8	-0.9	-0.1
FF	-10.1	1.9	-0.4

In the data above, “DH-1000”, “TC-155” and “HF-10” respectively refer to the damp heat test in 85°C/85% humidity for 1000 hours, the thermal cycling test for 155 cycles, and the humidity-freeze test. The results of the accelerated tests for thermal cycling and humidity-freeze are intended to simulate real-world conditions for product in the field, which is expected to undergo daily cycles in temperature and (potentially) cycles of freezing and thawing involving moisture in and around the package. The stresses imparted during these tests might be expected to impact module degradation through corrosion, or differential thermal expansion and contraction of different components in the module, leading to mechanical stresses on components and joints, particularly internal electrical connections.

Flexible Power Product - Testing and Reliability

Glass-based product more easily exhibits outdoor stability compared to flexible PV product, as the glass itself is impervious to moisture and oxygen ingress. However, potential degradation mechanisms do exist for glass-based product, and stability must be carefully evaluated to achieve the required 20-40 year service life. Outdoor field tests and accelerated tests are important to determine durability, failure modes and their causes.[3] Thus, testing requirements to assure stability for flexible product are yet more demanding. Additionally, flexible power product was

introduced more recently and development has taken place over a limited time during this subcontract. Despite this, significant progress has been made with good results indicated.

In initial approaches, several approaches for interconnecting cells were evaluated in outdoor tests for their application in flexible modules. Six modules of each stringing approach (A-C) were fabricated into ~7W, 10% efficient flexible modules; a standard GSE product design for flex product. The modules were deployed outdoors in early summer in Tucson. One group experienced extreme power degradation (C), a second group experienced rapid degradation followed by slow degradation to 85% of initial power (B), and a third group (A) varied somewhat during the period but generally maintained output without degradation (Fig. 1.7). The degradation of groups B and C was dominated by fill factor reduction. Analysis of the IV curves indicated that modules from groups B and C experienced increased series resistance. After 10 months outdoors, one of the stringing approaches, type A, continues to demonstrate stable performance. Modifications were made to the production processes to incorporate the important aspects learned in this test.

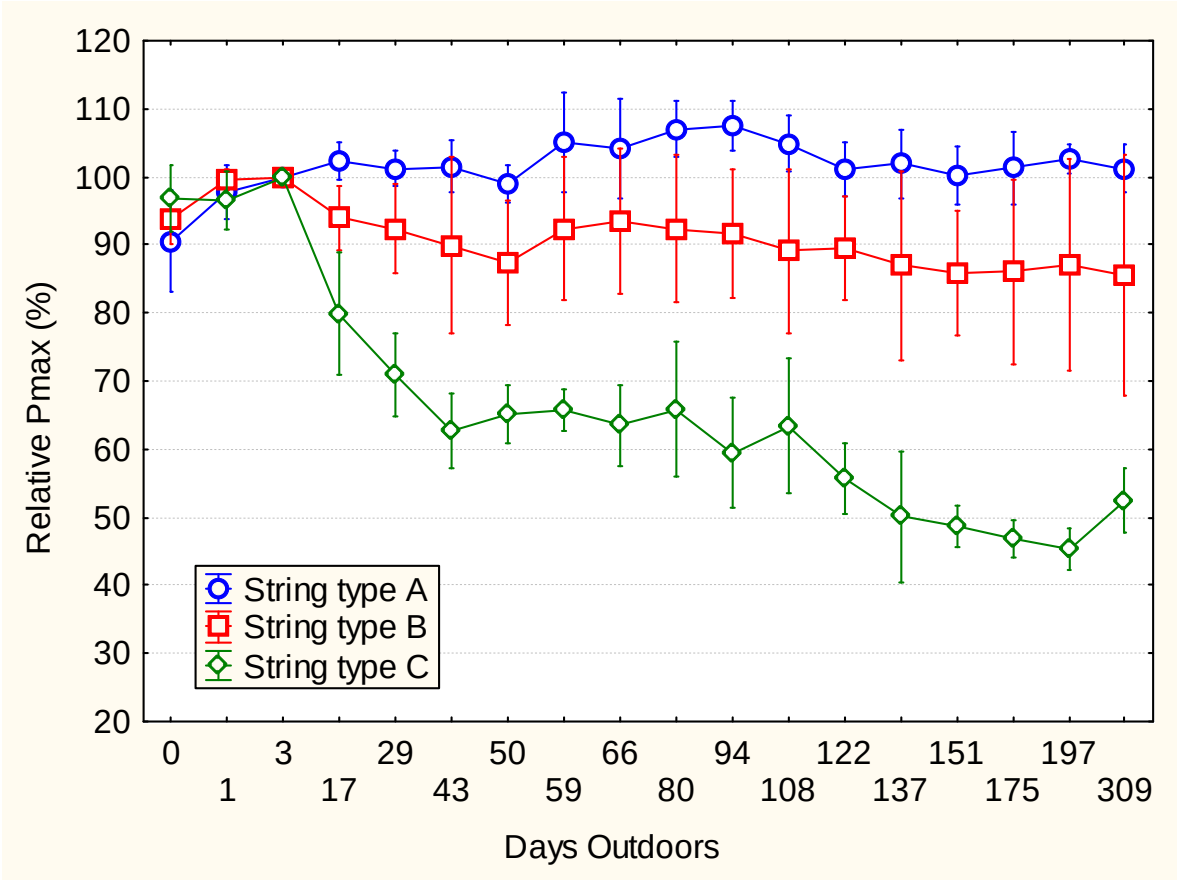

Fig. 1.7. Mean relative P_{max} of flexible modules fabricated by three stringing techniques and deployed outdoors in Tucson.

In other initial tests a transition to the larger 'Gen2' cells for flexible power product was studied to rule out special factors relating to that change alone. Accelerated testing was used on a comparative basis to look at GSE product made using larger "Gen2" cells vs. "Gen1" cells. Flexible modules were fabricated from Gen2 cells with the same packaging as a standard product

at GSE. Six modules were stressed in damp heat and six modules were deployed outdoors. The modules deployed in damp heat failed at a rate similar to the standard product fabricated from Gen1 cells. After 62 days outdoors, the other module set deployed in typical outdoor use still averages over 100% of initial power. Further time is required for any effects to become apparent. These types of tests eventually serve to build a link between accelerated and typical outdoor testing in terms of implied failure rates.

Although performance under "standard" conditions typically warrants the greatest study, some degradation mechanisms tend to show effects more rapidly at non-standard conditions. For example, failure mechanisms owing to increasing shunts in the PV product might be expected to impact weak light performance more rapidly than that under AM1.5 intensity. To identify any response of this nature, GSE fabricated modules using prototype Gen2 cells and characterized module performance at variable intensity before and after stress testing in damp heat. For exposure times less than 1000 hours, no significant change in the weak light module performance was observed.

Bending and peel strength tests take on much more importance in flexible as compared to rigid product. A multitude of ongoing study in these areas are underway. The peel strengths of various adhesives to materials applied inside CIGS PV modules were evaluated as a function of time in damp heat (85C, 85% RH). Two constructions using EVA films available from distinct suppliers (C and D), and another two using non-EVA adhesives with characteristics satisfactory for use in PV modules (A and B) were tested, results shown in fig 1.8. Peel test samples were prepared by laminating the adhesives to EVA-primed backsheets, PET, and Molybdenum-coated steel, and then separated using an Imada push/pull tester to pull on the prepared samples (Fig. 1.8). A strain gauge attached to the tester is used measure the force. The peel strength of EVA-bonded PET samples was found to drop significantly during the first several hundred hours of damp heat.

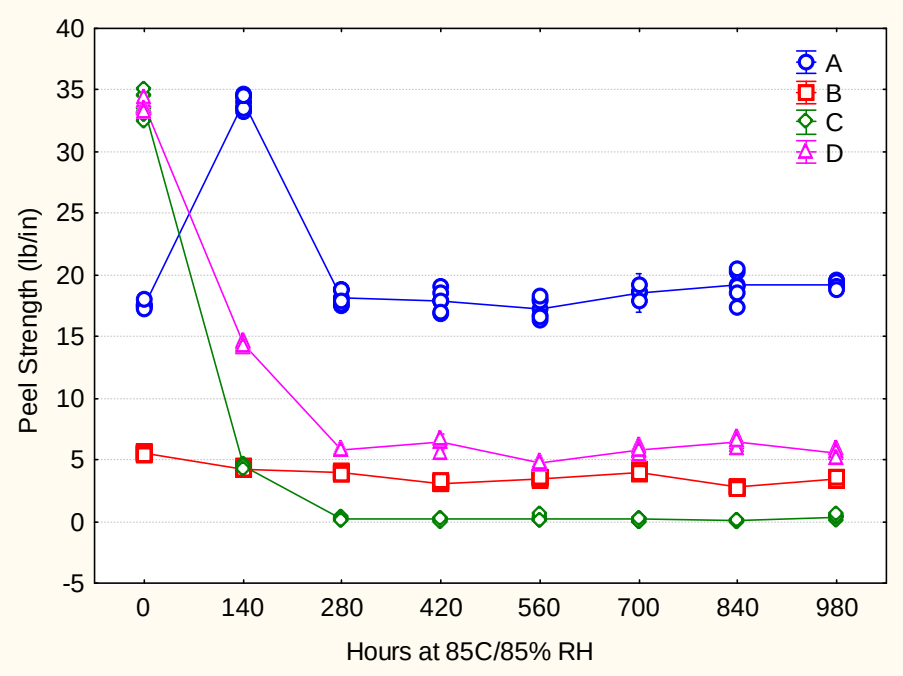

Fig. 1.8. Peel strength of various adhesives to PET film.

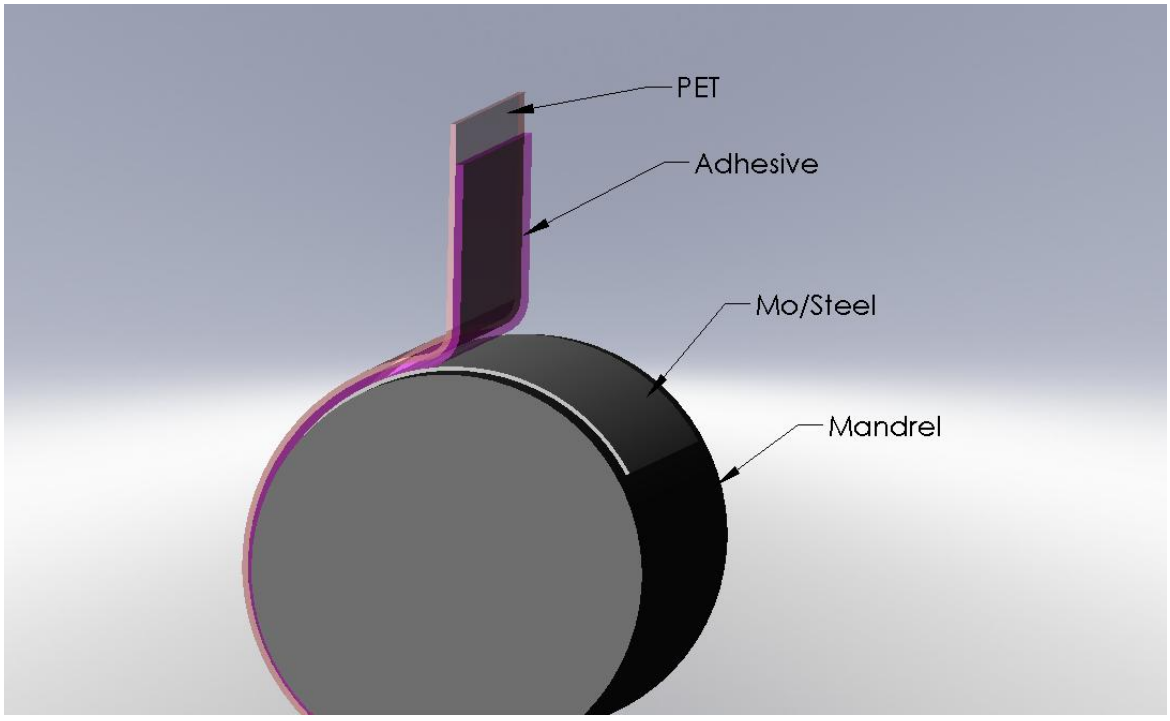

Fig. 1.9. Schematic of peel test set-up. The film is pulled vertically to separate from the substrate which is held on a mandrel. (Credit: Global Solar Energy)

Backsheet adhesion is also an issue requiring extensive testing. Several backsheets used previously with glass modules were evaluated for adhesion and module performance in damp

heat. The adhesion of the test backsheets to the standard adhesive was poor, and rapid damp heat test failure of those same backsheets in live modules was subsequently observed. Several items of note in these studies are that accelerated test results correlated to results in actual use, and materials that are successfully used in rigid power product are not necessarily applicable to flexible power product.

The frontsheet is more problematic, as materials having optical clarity with low water vapor transmission rates are desirable. In one study, transparent polymer films with coatings designed to act as water vapor barriers were received from multiple suppliers. The films were laminated over flexible CIGS solar cells (with leads attached) and subjected to damp heat stress and intermittent testing of the solar cells. Some of these initial results showed <20% degradation of P_{max} after 1000 hours, but further improvements in stability are necessary to enable a +20 year warranty.

Consequently samples of revised or alternate vapor barrier material were procured from four suppliers for another evaluation. Vapor barriers from three of the suppliers passed an adhesion peel test, and were subsequently evaluated in damp heat as the cover sheet for tabbed CIGS solar cells. An impermeable back sheet was applied to all samples opposite the “sunny-side”. At the end of the reporting period, two of the vapor barriers are showing encouraging performance compared to the control samples after several hundred hours in damp. Samples were stressed up to 2000 hours in damp heat before concluding the tests.

Many similar tests have been undertaken, and a multitude are ongoing presently for the flex power product. Reliability (as represented by stability in 85/85 conditions) continues to improve, with some recent results shown in fig. 1.10. The stability of the flexible CIGS product is evolving toward the level required for market acceptability more rapidly recently, owing to a better understanding of degradation mechanisms, appropriate test procedures, and also to an increasing availability of flexible polymer sheets incorporating vapor barrier layers.

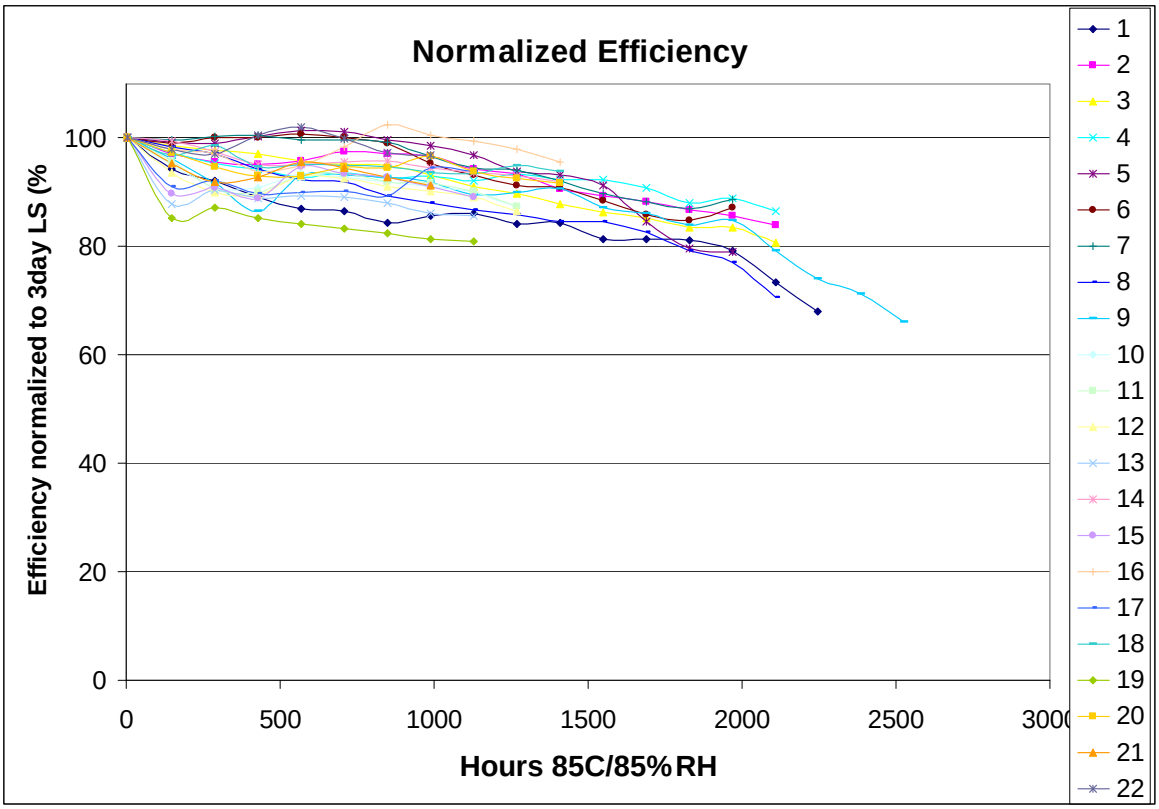

Fig. 1.10. Normalized efficiency vs time in 85°C, 85% relative humidity for a variety of CIGS module constructions. All modules use a flexible frontsheet, and over half shown above also use a flexible backsheet (the remainder use a glass backsheet).

Intrinsic Product Stability

One of the most remarkable aspects of CIGS product stability is that it appears to depend heavily on complex interactions between materials in most cases. As an example, although many module constructions have evidenced significant degradation in damp heat testing, instances have been noted of complete stability for naked (unprotected) CIGS cells exposed directly to the same damp heat conditions.

The relative efficiency of some unencapsulated small area devices as a function of exposure time in the 85-85 test is shown in Fig. 1.10. The devices were fabricated using standard GSE materials and processes, but consisted of only the device stack on the stainless foil substrate. Contacts for testing were made using evaporated metal grids with probes or indium solder.

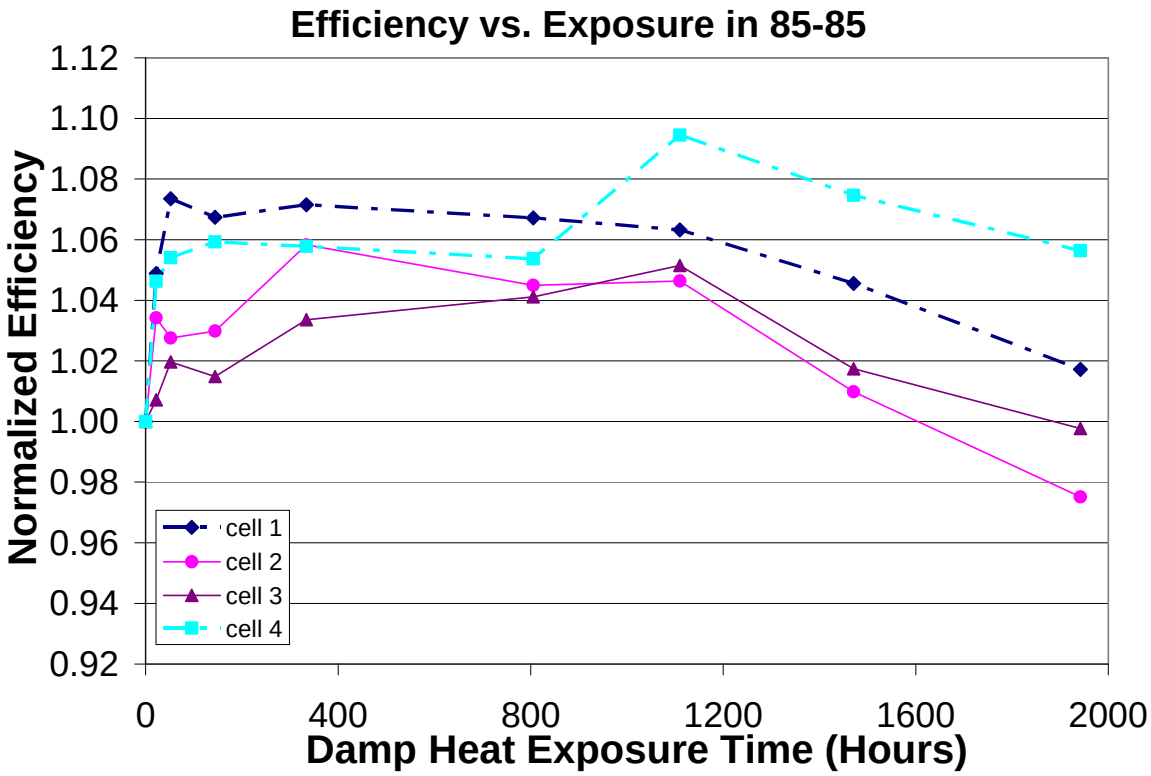

Fig. 1.11. Unprotected CIGS device efficiency (relative to starting efficiency) as a function of time exposed to 85°C / 85% humidity. These cells were completely unencapsulated during exposure and measurement.

This remarkable result indicates that the basic CIGS materials system, with heterojunction layer and front and back contacts of TCO and molybdenum on stainless foil, can be fundamentally stable. Thus it appears that many cases of observed degradation must be linked with other materials used in the module fabrication, or their interaction. Selective replacement tests in which various materials within the package are changed out with other materials clearly indicate the strong impact of the materials outside the thin film layers on the reliability of the total product.

Bending Tests for Flexible Power Product

Bending tests were designed to determine the bend radius below which cells are mechanically damaged, specifically at the junction between the printed fingers and the main collection buss. Gen1 cells (dimensions: 7.25 in. x 1.65 in.) with printed silver collection grid were bent around polished steel mandrels of decreasing diameter. Cells were oriented with the collection fingers perpendicular to the axis of the steel mandrel. To avoid non-uniform stress, the force required to conform the cell to the mandrel was applied through a silicone foam rubber.

Cells were tested in both compressive (grid toward mandrel) and tensile stress (grid away from mandrel). Controls were re-measured along with each of the two stressed sets to rule out

potential effects of repeated measurements. There were ten samples in each of the stressed groups and five control samples.

The results, shown in Fig. 1.11, indicate that compressive stress results in greater damage than tensile stress for a given bend radius. Little or no damage was apparent for either stressed group down to a bend diameter of 0.25 inches. The controls changed little during the duration of the test.

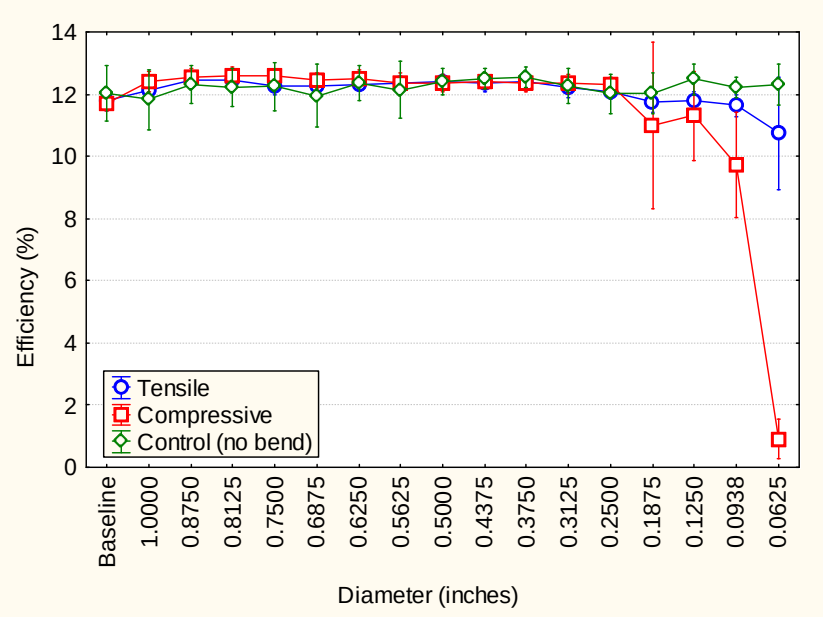

Fig. 1.12 Mean efficiency of cells after being bent around mandrels with decreasing diameter.

Improved Product Appearance, Uniformity

Color variation of the CIGS cells, which is primarily due to thickness variations in the CdS layer is of concern for aesthetic considerations. Efforts to improve the control and uniformity of key variables, including reactant introduction in the CdS process resulted in significantly improved CdS uniformity and process control. The more uniform appearance in finished product that resulted is evident in the comparison of product photos in figures 1.12 and 1.13 below.

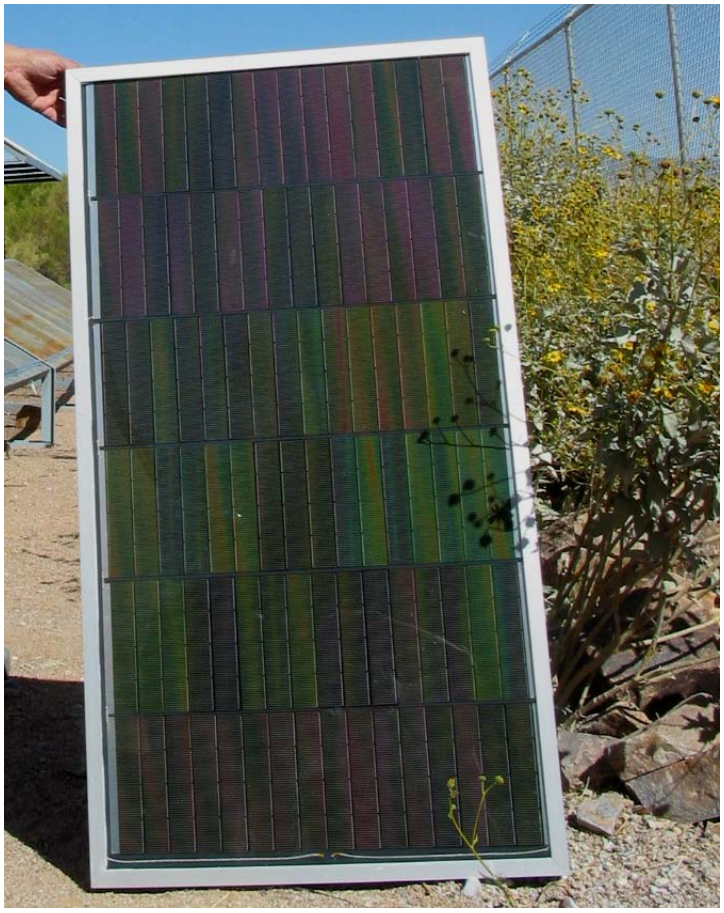

Fig. 1.13. An early large area product based on the Gen1 cell fabrication, and showing typical color variation due primarily to thickness variation in the initial CdS process. (Credit: Global Solar Energy)

Fig. 1.14. A color photo of more recent large area product based on the Gen2 cell fabrication, and showing the more uniform color appearance attained with improved control of the CdS process. (Credit: Global Solar Energy)

After these improvements the CdS thickness variation appeared not to exceed limits required for good electrical performance. However, more careful measurements of quantum efficiency made at NREL subsequently indicated that a variation in electrical performance that was linked to the CdS layer (see Fig. 1.14). An analysis of the QE in the wavelength range near 460 nm done at NREL indicated that the CdS thickness may vary from 360Å to 700Å, which was correlated with variation in local J-V parameters (specifically Voc and FF). Thus, despite the improvement in uniformity, it appears that further improvements in uniformity would be beneficial.

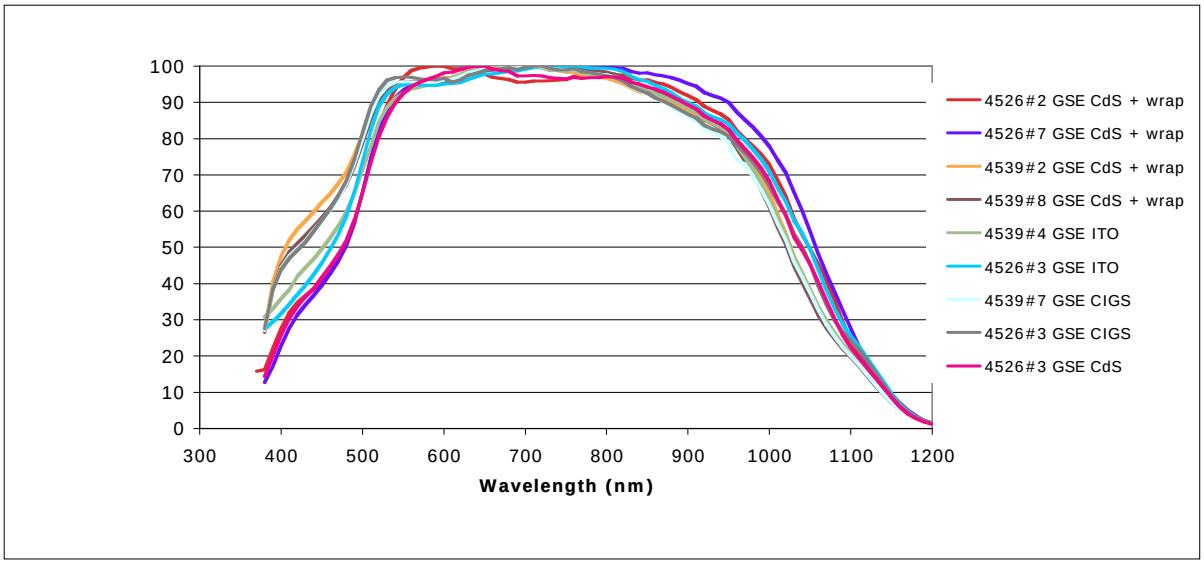

Fig. 1.15 Relative QE measurements on GSE samples made at NREL showing variation in the wavelengths near 460 nm where variation due to CdS thickness changes would be prominent.

Task 2: CIGS Coating Cost Reduction (Objectives)

1. Increase processing rate for CIGS deposition by at least 25% with a high-bar goal of 50% (from 12-in/min to 15-in/min and potentially 18-in/min).
2. Modify effusion sources as necessary to ensure adequate cross-web uniformity at increased absorber formation speeds.
3. Reconfigure In and Ga sources to allow improved homogenization of In-Ga at the higher CIGS deposition rates and reduced time for mixing by diffusion.
4. Re-optimize CIGS process parameters for device efficiency at the high processing rates and altered In-Ga delivery.
5. Evaluate alternate sodium delivery, for efficiency, control and uniformity; and high process rates, implement if successful into the standard process.
6. Evaluate thinner CIGS layers. Reduce flux rates to achieve less than 1.0 µm CIGS thickness and re-optimize CIGS process conditions to maximize efficiency for thin absorber layers.

Production Scale-up (New Manufacturing Facilities)

Since the overall intent of this contract is to enable significant gains in cost and throughput for thin film PV, and “economies of scale”, coupled with improved capability in production equipment are key to those goals, we will report on changes impacting these factors here. The specific process improvements to enable significant cost and throughput gains are listed in the objectives above (for the CIGS layer, and in the following sections for the front and back contact layers). However, the overall contract goal and many of the specific process improvements are related to, or dependant on, the design and installation of improved plant and equipment. In

2006, GSE was charged with expanding its manufacturing capability by more than an order of magnitude. GSE was expected to bring on line a new plant (in Tucson), with re-designed equipment for all processes within 12 months. Subsequently, another plant in Berlin, Germany having a capacity of 35 MW/year was planned in addition to the 40 MW/year capacity slated for the Tucson plant.

During phase 1 of this TFPPP subcontract GSE located and negotiated the purchase of a building and land (110,000 sq. ft., and 22 acres, resp.) in Tucson, and made lease arrangements for the factory space in Berlin. The Tucson building was formerly one of the largest magnetic tape coating facilities in the world, so in this sense the new PV factory continues the thin film coating legacy of the original building. Other similarities are absent, and thus the interior of the former building was entirely demolished, and then rebuilt. All existing equipment was removed, an extensive volume that filled a 250,000 sq. ft. lot 3 times over. Industrial architects and contractors were engaged to plan all aspects of the new plant – renovation, distribution of utilities such as electrical power, compressed air, process gasses, chemical distribution and containment, process cooling water, heating, ventilation and air conditioning, humidity control, storage and office space. Figures 2.1-2.5 below show the Tucson facility in early stages of demolition.

Fig. 2.1. One section of the GSE Tucson building under demolition. (Credit: Global Solar Energy)

Fig. 2.2. A northeast section of the GSE Tucson building under demolition. (Credit: Global Solar Energy)

Fig. 2.3. The building exterior for the Tucson facility before renovation. (Credit: Global Solar Energy)

Fig. 2.4. Interior structures, equipment chases and HVAC under renovation in the Tucson facility. (Credit: Global Solar Energy)

Fig. 2.5. Interior rooms, overhead lighting and HVAC under renovation in the Tucson facility. (Credit: Global Solar Energy)

Simultaneously, subcontractors were engaged to design and build deposition and production equipment for all the processes required for large scale CIGS PV manufacture. Deposition equipment was built to GSE specifications and concepts, based on the actual manufacturing experience GSE had gained with the 1st generation equipment at the existing plant in Tucson. In all cases, the re-designed equipment embodied advancements, including:

- Deposition equipment built for higher deposition rates,
- Reduced product cost,
- Improved materials utilization,
- Enhanced process control and reproducibility,
- A high degree of automation, all processes are designed to run largely unattended,
- High throughput,
- Process flexibility.

Specifically for the CIGS process, the deposition equipment was designed to handle rolls of substrate 3x the length of the existing, 1st generation equipment, at 2x the speed, with better cross-web and down-web uniformity, improved In, Ga and Se utilization, and more process flexibility.

Economy of Scale – Factory Completion

As scalability is a key advantage of the thin film approach, particularly using the roll-to-roll processes for thin film coating that GSE has pioneered, overall cost reduction is heavily dependent on factory scale-up to significant size. During the 2nd phase of this Thin Film Partnership subcontract substantial progress was made toward completion of the GSE plants in Tucson and Berlin (40 MWp and 35 MWp capacities respectively). A rough chronology of major events throughout the 2nd phase include:

- Further required planning and construction of the GSE production facilities in both Tucson and Berlin and related equipment were carried out concurrently, saving time but increasing risk.
- Demolition of the Tucson (Rita Road Site) 103,000 sq. ft. building interior was completed.
- Construction of the new interior started on 6/15/2007. The objective was to prepare the facility for installation of new tools that began arrival in October. Building completion was staged to accommodate the tools as they arrive.
- The building was completed generally from north to south, shown in Fig. 2.6, with temporary barriers erected to separate active construction areas from completed areas receiving production tools.
- Facilities such as chilled water, compressed air, electricity, exhaust, and air conditioning were brought up and distributed dynamically as required for the production tools as they arrived.

- Production tools were generally checked and accepted once at the suppliers' sites and then checked and accepted again after final installation at GSE (either Tucson or Berlin).
- Production tools were installed and facilitated as they arrived from diverse fabricators. Complete sets of thin film coating equipment (back contact, absorber, heterojunction formation and front contact roll-to-roll coating tools) were operational midway through phase 2 (examples shown in Figs. 2.7 and 2.8).
- Transfer and development of the process for the thin film coating steps was initiated (back contact, absorber, heterojunction and front contact steps), concurrently with the installation of additional tools. For instance, the majority of the hardware for the first installed CIGS system (CIGS5) was demonstrated to be robust, reliable and proven capable for depositions extended to 600m web lengths while the second system (CIGS6) began installation.
- Remaining process tools were installed and qualified, including tools for printing, slitting, "tabbing", "stringing" and measurement functions.
- Evaluations were conducted as necessary to successfully increase web lengths from 300 meters to 600 meters in length, from 12.5" to 13" in width and from the smaller "Gen1" to the larger "Gen2" cell format. All of these changes capitalize on the economies of scale built into the design of the new factory processes and equipment. An equipment integration plan required the Gen2 processes to be individually qualified against Gen1 processes with known metrics. Wherever the approach required web interchangeability between the old and new production tools, modifications were made to the Gen1 equipment to allow it to process the wider web.
- Tests were conducted in CIGS deposition tools to determine the accuracy of the in-situ sensors and develop the control parameters that lead to CIGS with characteristics similar to the films deposited in the Gen1 production line. All deposition tests were conducted at a web speed of 0.61 m/min (24 inches/min). The metrics evaluated for these first optimizations were coating thickness, composition, adhesion, morphology, visual appearance, and solar cell performance. Initially, achieving a sufficient and controllable supply of selenium was a notable problem.
- Cell performance was evaluated by applying other coatings (besides CIGS) in the Gen1 line, and fabricating Gen1 cells ($68cm^2$). By the fourth such test, gross control set points had been derived that resulted in a maximum efficiency of 8.6%.
- Ongoing efforts were then focused on 'Gen2' processes and form factors for continuing process optimization of the thin film and other factory processes, increasing measured cell efficiencies and reproducibility, and thus yield.

Fig. 2.6. The new GSE manufacturing facility in Tucson (10,220m^2). (Credit: Global Solar Energy)

Fig. 2.7. A GSE tool for roll-to-roll absorber (CIGS) deposition at the new manufacturing facility in Tucson. (Credit: Global Solar Energy)

Fig. 2.8. Roll-to-Roll equipment for one of the "back-end" processes in the new factory (front contact collection grid printing). (Credit: Global Solar Energy)

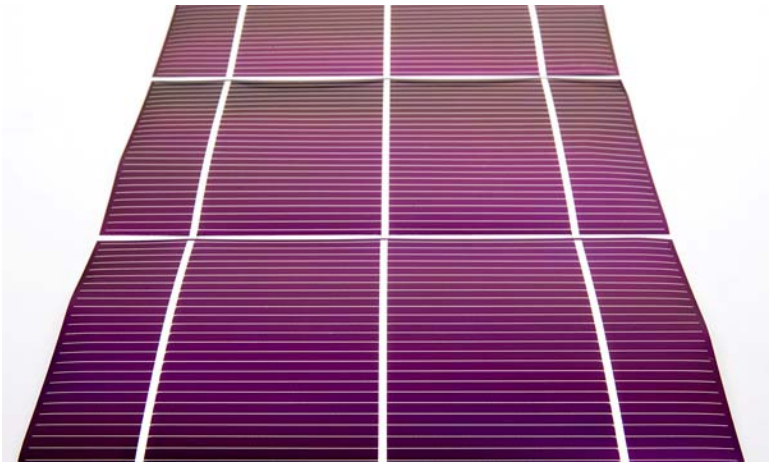

P_{mp} (W):	39.5
V_{mp} (A):	7.3
I_{mp} (A):	5.4
V_{oc} (V):	10.3
I_{sc} (A):	6.7

Fig. 2.9. A view of the thin film CIGS-based PV strings on metal foil (and nominal string electrical characteristics) that represent the initial' Gen2' product of the new GSE factory. (Credit: Global Solar Energy)

Enhanced CIGS Deposition Rates

For CIGS formation the maximum rate possible is hitherto unknown, being limited at some point by the time-at-temperature required for sufficient materials reaction and diffusion through the absorber layer thickness. High CIGS formation rates are desirable to maximize throughput for the CIGS deposition, and is one of the goals of this program. Limited CIGS deposition speed trials were run early in this TFPPP program, demonstrating that deposition speed can be increased from 12 to 15-in/min in the 'Gen1' equipment without any impact on performance or material characteristics. Absorber layer compositions evaluated with Auger electron spectroscopy indicated essentially no change in the desired profile at 15-in/min compared to 12-in/min in Fig. 2.10.

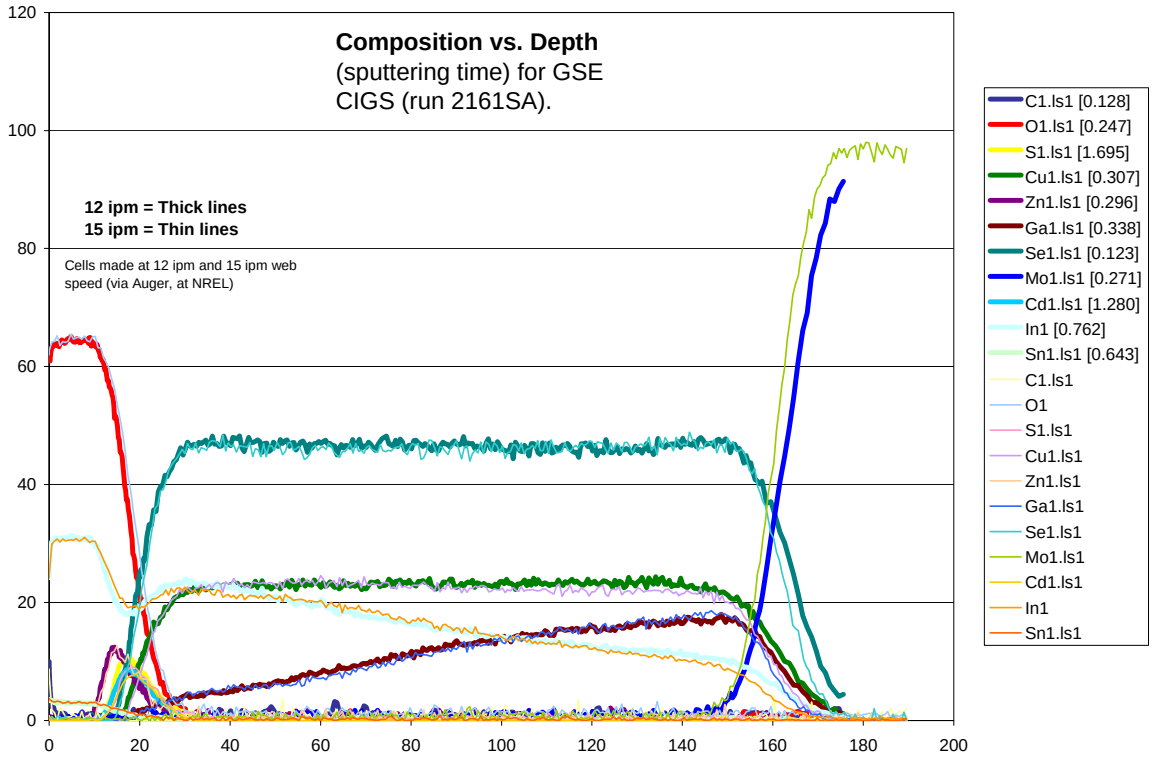

Fig. 2.10. Auger electron spectroscopic analysis done at NREL comparing the composition of cells made at GSE at web speeds of 12 and 15-in/min on 'Gen1' equipment.

With proper control adjustments to flux rates at different stages of deposition, it is apparent from Fig. 2.10 that the deposition rate (and web speed) can be increased by at least 25% over the standard rate for the Gen 1 process at GSE while maintaining a virtually identical composition profile. More importantly, 'Gen1'cells made at the 15-in/min speed were equivalent in performance to those made at the 12-in/mid CIGS deposition rate. Representative electrical data for a large area 'Gen1' cell made at 15-in/min is shown in Fig. 2.11.

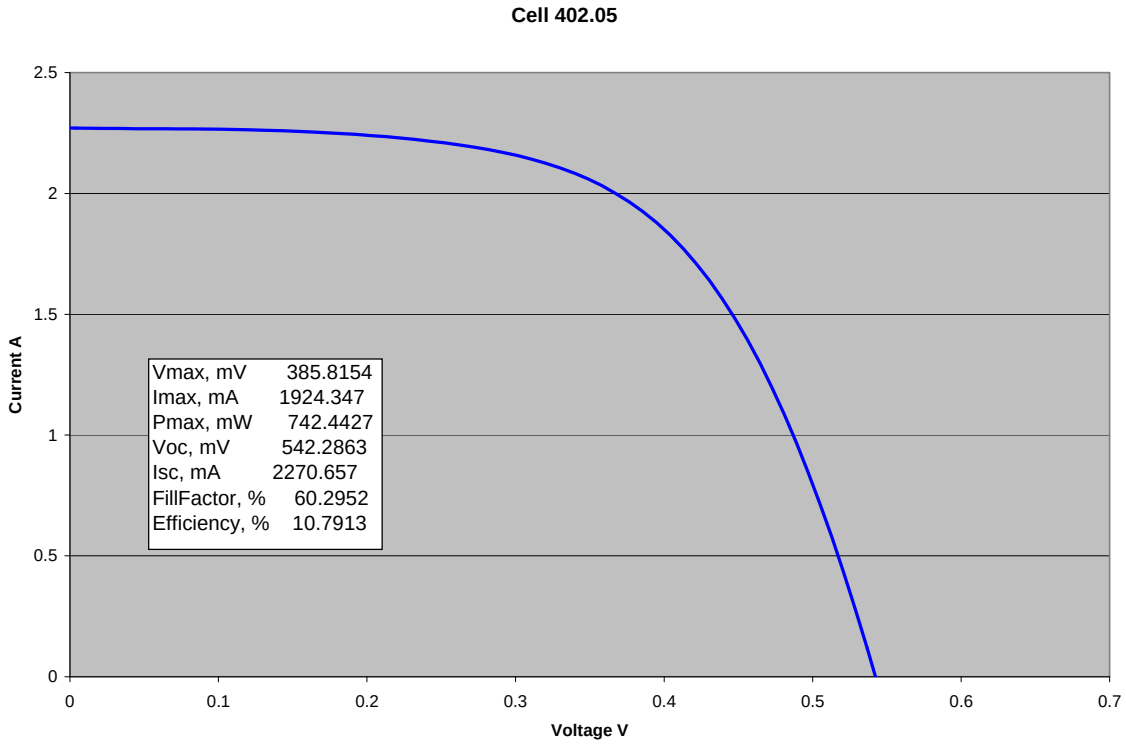

Fig. 2.11. ***A representative I-V characteristic for a large area cell made at an increased web speed of 15-in/min on the 'Gen1' equipment.***

Upon moving to all 'Gen2' equipment in the new plants, cost reduction in the CIGS process (and other processes) was largely addressed through improvements to equipment design, process control, engineering, operational procedures and process setpoints that were all directed toward running at higher deposition rates, and for increasing web lengths. In addition, the 2nd generation equipment was designed to allow more control and flexibility over the composition profile, further enhancing possibilities for achieving even higher deposition rates and/or performance. High deposition rates and increasing web lengths are effective in reducing cost, but only if cell efficiency and yield can be maintained concurrently. Internal goals called for increasing web length to 1 km through all tools, with CIGS deposition rates of between 19 and 24-in/min.

CIGS deposition rates in this range were evaluated for the impact on solar cell electrical characteristics. In the test, the deposition rate was varied by moving the web at two different speeds (51 and 61 cm/minute) and adjusting the effusion source fluxes at each web speed to supply identical thicknesses of Cu, In, and Ga. Diffusion was not controlled in this test since the web temperature is dependent on residence time near heating sources (including the effusion sources).

Gen1 cells (area: 68cm^2) were prepared on panels extracted from each test region. Mean electrical characteristics for each web speed are shown in the table 2.1. Cells with CIGS deposited at the lower web speed exhibited higher efficiency, primarily due to higher fill factor.

Table 2.1. Mean electrical characteristics of cells with CIGS deposited at 51 and 61 cm/minute.

	CIGS at 51 cm/min.	CIGS at 61 cm/min.
Voc (mV)	569	566
Isc (mA)	2183	2194
Fill Factor (%)	55.7	53.5
Efficiency (%)	10.5	9.8

This and other tests indicated that good efficiency could be attained while meeting the internal goals of between 19 and 24-in/min. All 'Gen2' results cited henceforth were achieved at a CIGS deposition rate of 20-in/min, unless otherwise noted. This CIGS deposition rate exceeds both the goal and "stretch goals" of the TFPPP program of 15 and 18-in/min respectively.

Fundamental improvements were also made in the design phase for the 2nd generation equipment to address the 2nd, 3rd and 4th objectives listed in this task. Significant changes to the effusion source design used for CIGS deposition were made to ensure adequate cross-web composition uniformity, in addition to improvements in materials utilization. This objective was complicated by concurrent demands for operation at higher deposition rates (discussed above) and greater capacity demanded by the planned introduction of much longer runs for up to 3x length webs in the 2nd generation equipment.

Improvements in In-Ga homogenization and compositional profile control, and performance improvements relating CIGS processing parameters (per the 3rd and 4th objectives) have been addressed by instituting a scheme for more flexible delivery of CIGS reactants, but also requires optimization to find the optimal delivery profile. Steady progress has been made in this regard leading to increasing efficiencies and yields for the large area 'Gen2' cells.

Absorber (CIGS) Deposition Process

Successful CIGS deposition invokes a multidimensional parameter space that must be well understood and well controlled. Multisource co-evaporation offers perhaps the greatest flexibility and potential in device engineering on an atomic level. This potential comes at the cost of severe engineering challenges in scaling a process requiring multivariate control under extreme conditions in a harsh and difficult environment.

Compositional control and uniformity of copper, gallium and indium is crucial to achieving product performance and yield. Cross-web uniformity is governed chiefly by the design and control of the effusion sources and the geometry of the deposition zone. Down-web compositional uniformity is more a function of temporal control - stability of the effusion sources and efficacy of the real-time process monitors and closed-loop control algorithms. In the design of the equipment for the new factories, GSE intentionally increased the degrees of freedom and also designed the systems for higher deposition rates and capacities. These factors presented further challenges in the engineering, and in the process development. At the end of

the second phase, GSE had demonstrated satisfactory control and uniformity in CIGS composition, as shown below. Nonetheless, further improvement is anticipated in these areas. A typical cross-web composition is shown in Fig. 2.12. for the CIGS deposition equipment at the new GSE factories operating at a 61-cm/min web rate.

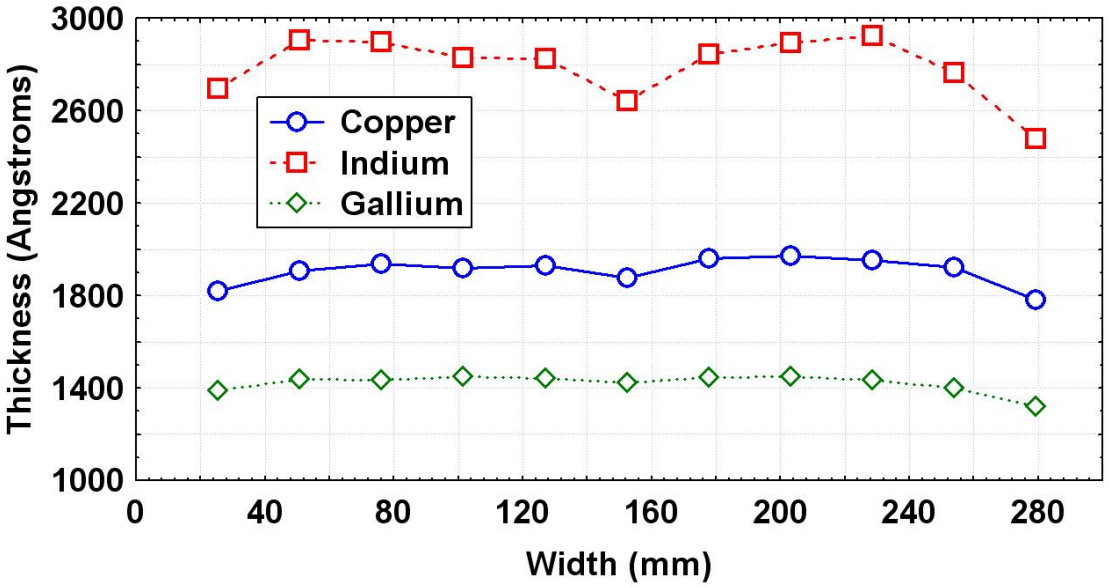

Fig. 2.12. Equivalent thicknesses of copper, indium, and gallium in a typical CIGS film (across the web width) as measured by ex-situ XRF.

Fortunately, compositional ratios of Cu/(In+Ga) and Ga/(In+Ga) are more critical than absolute equivalent thicknesses of the individual elements, or than total thickness of the CIGS layer itself. These quantities are plotted in Fig. 2.13 for the same web in Fig. 2.12.

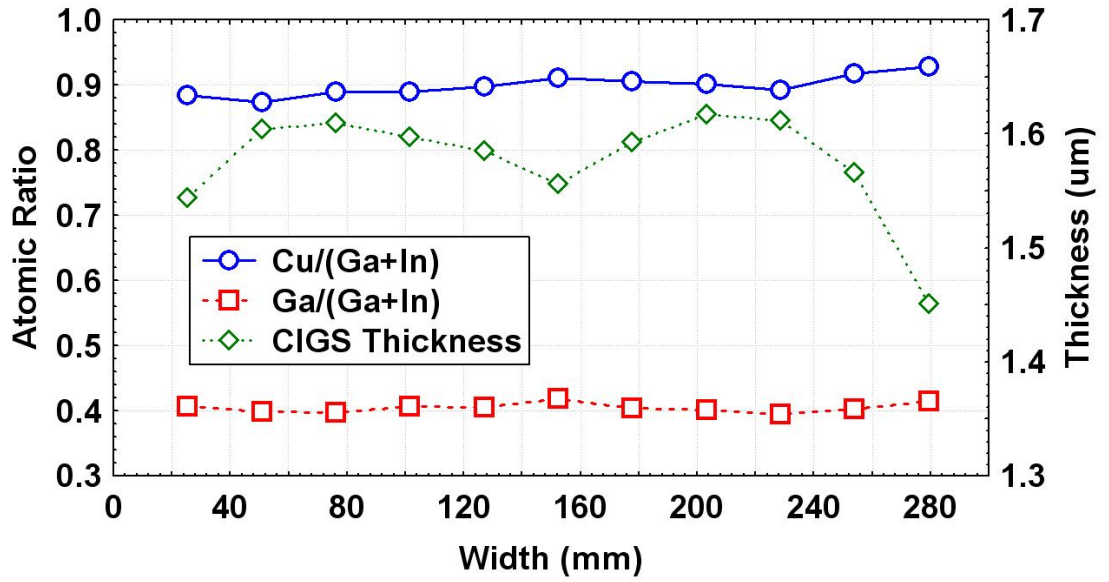

Fig. 2.13. Atomic ratios and total thickness of a CIGS film (across the web width) as measured by ex-situ XRF.

Considerable effort in process control methods at GSE have resulted in uniform compositional control both across and down-web at the high web coating rates required. Fig. 2.14 shows the equivalent thicknesses for copper, indium and gallium as a function of down-web location for a typical deposition.

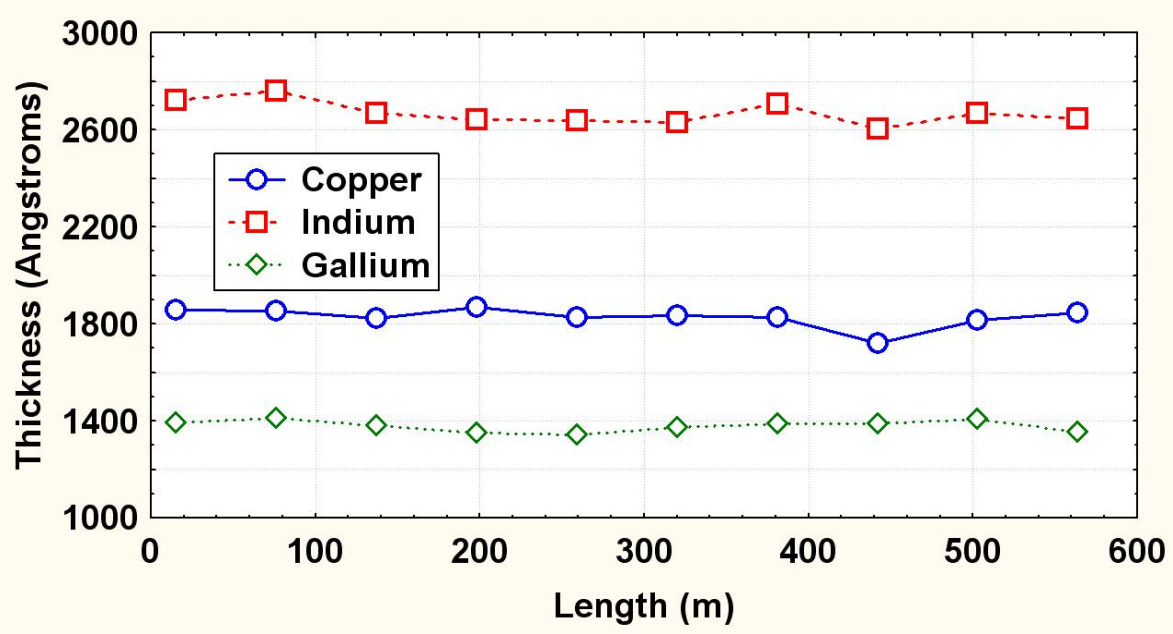

Fig. 2.14. ***Equivalent thicknesses of copper, indium, and gallium in a typical CIGS film (down the web length) as measured by ex-situ XRF at the web center.***

The forgoing also illustrates the importance of process monitoring tools. Consequently, upgrades were made to the XRF software and calibration to improve measurement accuracy. Greater accuracy in measuring Cu, In, Ga, and Mo enables better process reproducibility, and is required to optimize the absorber band gap with fine detail. Fig 2.15 shows the discrepancy in the elemental layer thickness (for Cu, In, Ga and Mo) between measurements of the same film made at different machine locations and in different machines. Results are shown before, and after the correction upgrades were added to the algorithms. Before the correction upgrades the measured elemental thicknesses at a 2nd location were consistently less than at the first location, and could disagree by 10-15%. After the upgrades to correct measurement errors automatically the same measurements typically differed by 2-5%, with an error more uniformly distributed about zero. These measurements were made “real-time” under “hot” or actual deposition conditions.

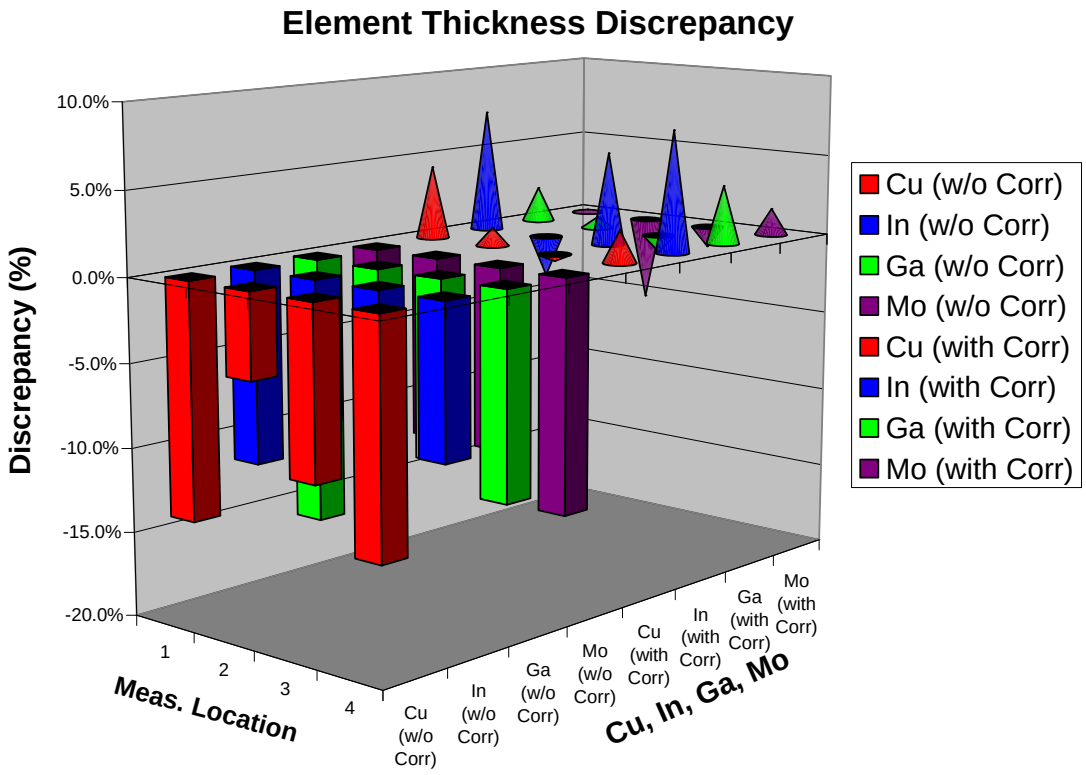

Fig. 2.15. Discrepancy in the elemental layer thickness (for Cu, In, Ga and Mo) made in several locations before (square columns) and after (cones) upgrades were made to automatically correct measurement errors in XRF real-time readings.

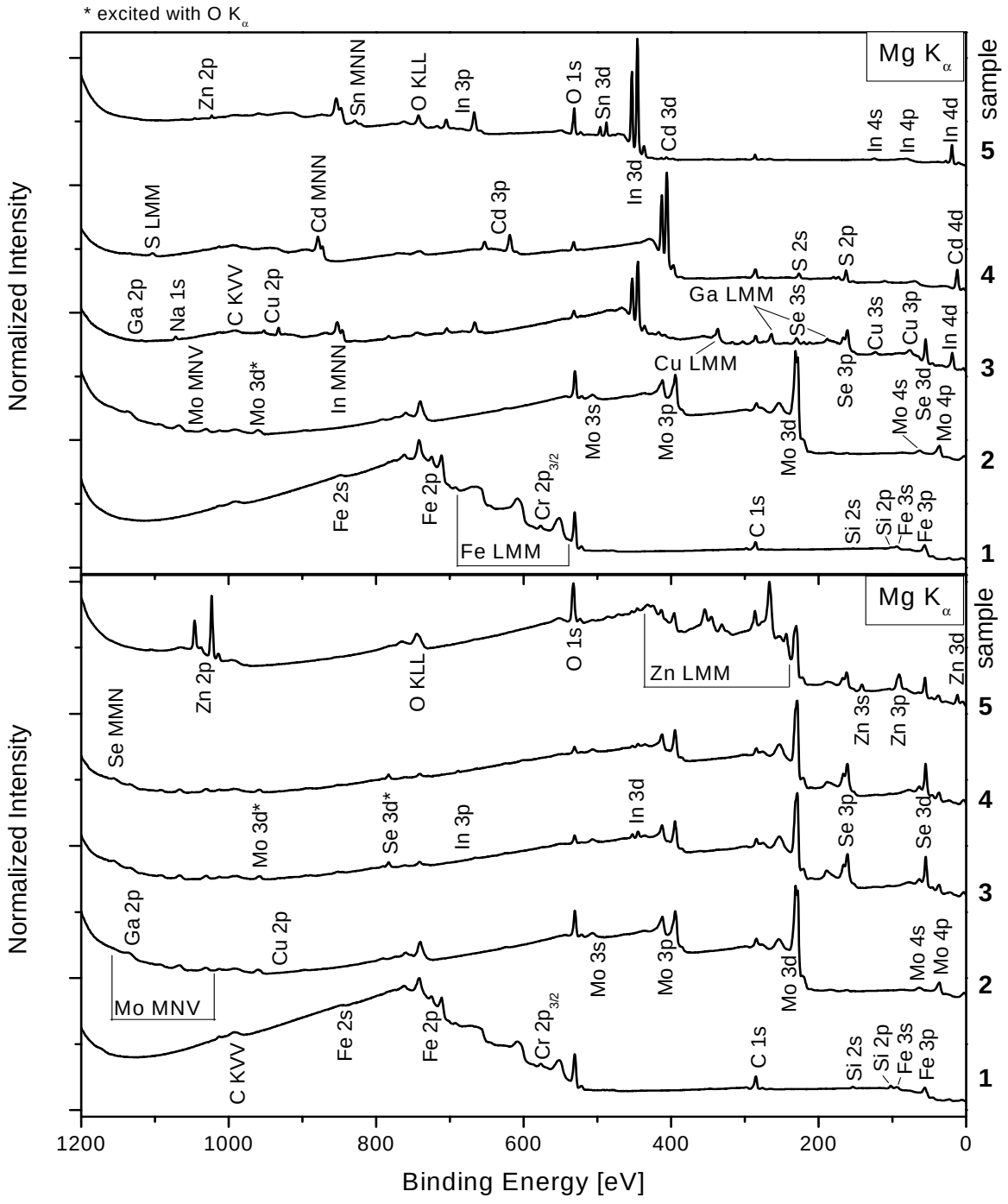

Fig. 2.16. XPS survey spectra of the front (top panel) and back side (bottom panel) of the investigated test structures.

In optimizing process setpoints, including processing rates and temperatures, it is useful to gain as much insight into the materials interactions as possible. For instance, it is important to understand the state of the starting substrate, Mo-coated stainless foil, in terms of its composition, contamination level, oxidation, tendency toward selenization as the process proceeds, etc. Knowing the relative changes in interfaces throughout the device under "standard" processing conditions allows better interpretation of how changes made to increase reaction rates might impact important interfacial reactions. Toward that end, through collaboration with the laboratory at UNLV directed by Dr. Clements Heske, GSE has obtained data on the surface condition at important steps in the device formation process using XPS. This data was obtained as a 'baseline' for standard conditions on both the front and backside of the substrate, shown in Fig. 2.16.

More detailed interpretation of the meaning of the data is given by Dr. Heske in his report of 5-2008 to NREL under the TFPPP initiative. The data indicates some conversion of oxides of moly to selenides during processing, and the transport of some constituents of the CIGS deposit to the backside of the substrate.

Absorber Thickness Variation

The sensitivity of the solar cell electrical characteristics to CIGS thickness was also evaluated on a continuous 330 m web. In this test, the film thickness was varied by moving the web at two different speeds (51 and 61 cm/minute) while maintaining constant effusion source fluxes. The deposition rates are identical, but the coating deposited at the lower web speed likely reached a higher temperature from increased residence time near heating sources. This simple test approach leads to a "stretching" of the entire band gap profile in the thicker film.

The CIGS coating thickness for the two test conditions was evaluated by XRF. The mean thicknesses for the "thin" and "thick" coatings were 1.31µm and 1.69µm, respectively.

Gen1 cells (area: 68cm^2) were prepared on panels extracted from each test region. Mean electrical characteristics for each coating thickness are shown in the table 2.2. Cells with thicker CIGS exhibited significantly higher efficiency, with all electrical parameters improved.

Table 2.2. Mean electrical characteristics of cells with "thin" and "thick" CIGS

	"Thin" CIGS	"Thick" CIGS
Voc (mV)	566	580
Isc (mA)	2141	2275
Fill Factor (%)	54.5	58.3
Efficiency (%)	9.7	11.2

These results indicate that further effort, likely involving significant changes to deposition conditions and composition profile will be required to achieve comparable efficiency cells with the use of thin absorber layers.

Alternate Na Incorporation

One alternate method for Na incorporation was completed through an initial evaluation. The benefits of this alternate method over the standard operating process ('SOP') would potentially be better dose control, better uniformity, improved yield and adhesion. A first experiment used one manufacturing lot to compare the standard method to the alternate method and also to no Na introduction (fig 2.17).

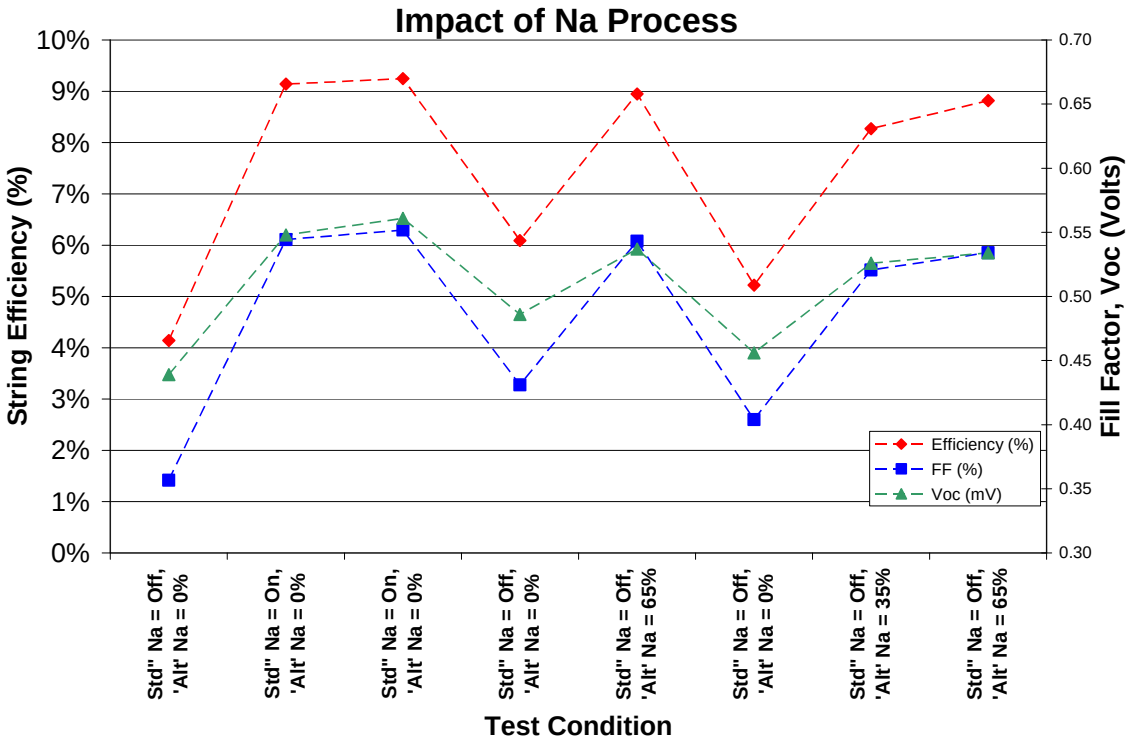

Fig. 2.17. Average efficiency, fill factor and Voc of "strings" of full sized Gen2 cells produced using 2 different methods of Na incorporation, or none at all. The strings were fabricated using standard manufacturing techniques otherwise, and consisted of 18 serially connected large area cells (210 cm^2) each.

The data reiterates the importance of Na incorporation, and indicates that either the standard or the proposed alternate methods are effective. The varying levels of Na used with the alternate technique suggest that a level of Na above 35% (arbitrary units) is required.

A second experiment using mostly "Gen2" process steps and equipment, with augmentation or replacement of one step using modified "Gen1" equipment was conducted. Sodium incorporation was accomplished using the standard process, the alternate process (with varying quantities), and both processes, with results in fig 2.18, allowing a finer comparison of the two approaches.

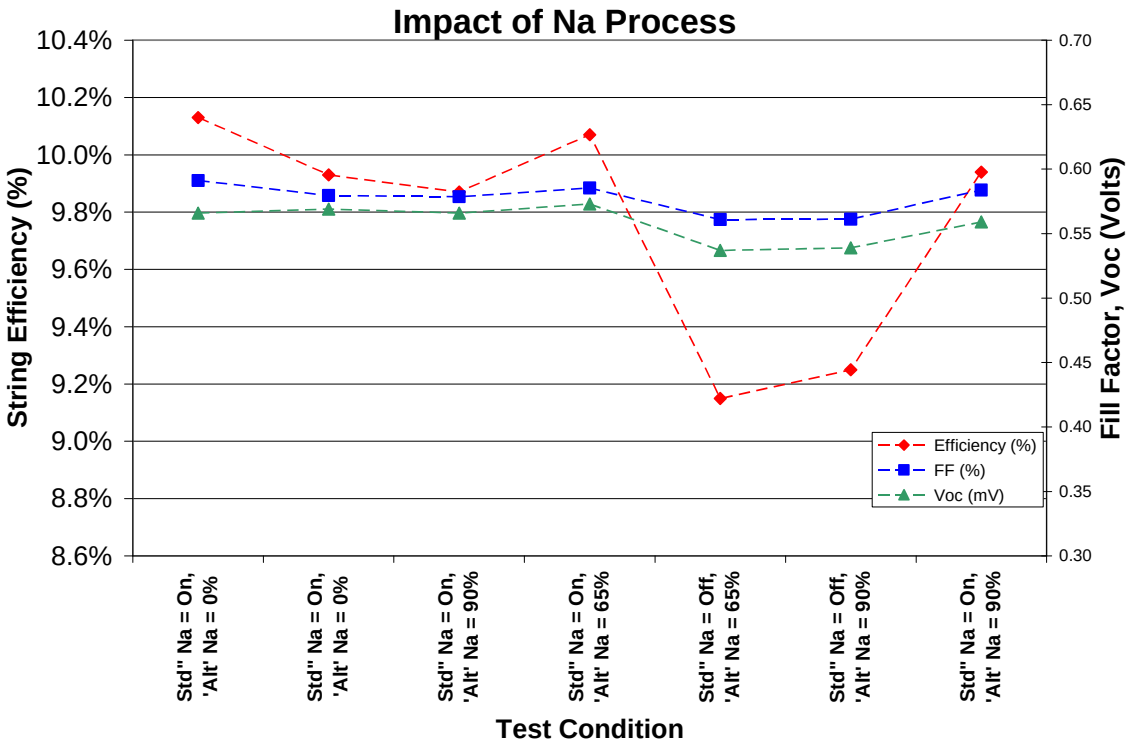

Fig. 2.18. Average efficiency, fill factor and Voc of "strings" produced using two different methods of Na incorporation, or both simultaneously. The strings were fabricated using standard manufacturing techniques otherwise, and consisted of 18 serially connected large area cells (210 cm^2) each.

This data indicates that, although the alternate Na incorporation process is effective, the cell and string performance does not match the standard process for Na incorporation. Again, the loss in efficiency stems mostly from fill factor and Voc, as would be expected, and amounts to almost 1 percentage point in efficiency between the two methods. Additional Na or a combination of both Na incorporation methods does not improve results above the standard process alone. In this first test appropriate quantities of Na for the alternate method were estimated, and may not have been high enough.

Thermal Coefficients for IV Parameters and "Bandgap Engineering"

Thermal coefficients for IV characteristics were measured for glass modules fabricated from Gen2 strings. The evaluations were conducted outdoors under cloudless conditions. A portable IV tester, calibration cell, and a transparent window box (to limit wind cooling) were utilized. Module temperature was monitored by an adhesive thermocouple attached to the back of the module. Utilizing specially-fabricated structures, tests were conducted to determine the temperature differential between a thermocouple mounted directly on the back of the string and the exterior surface of the backsheet. The difference was found to be less than 2°C. Average thermal coefficients are shown in Table 2.3.

Table 2.3. Thermal coefficients for Gen2 strings in glass modules.

Vmax (%/C)	Imax (%/C)	Pmax (%/C)	Voc (%/C)	Isc (%/C)	FF (%/C)
-0.49	-0.13	-0.59	-0.39	0.03	-0.24

The figures above pose an opportunity for enhanced power generation under field conditions where module temperatures are typically higher than 25°C dictated by STC conditions. Work started in 2010 to increase the effective bandgap in the active region of the absorber, thereby reducing the performance loss with increasing temperature. The CIGS materials system is tolerant to bandgap modification over a substantial range[4] via gallium or aluminum substitution for indium, or sulfur substitution for selenium. Higher open circuit voltage is attained, usually at the expense of short circuit current, so that if fill factor can be maintained, there may be no loss in overall efficiency.

Even without any efficiency gain at STC, increasing the bandgap provides two benefits: a higher voltage with less current reduces I^2R losses, and a higher bandgap material exhibits a reduced rate of power loss versus temperature. This latter effect is significant for operation in most climates where actual cell operating temperature is much above standard measurement conditions of 25°C. Figure 2.19 shows the variation in the temperature coefficient for power measured on large area cells whose CIGS bandgap had been changed by modification of the Ga content.

Using the linear relationship derived from a fit to the data of figure 2.19 the reduction in efficiency at elevated operating temperature can be estimated. The cell operating temperature was calculated using methods outlined by D.L. King[5] for a location in the southwest US at 980 W/m^2 irradiation for conditions representative of operation at mid-day in April and June (corresponding cell temperatures of 49.5°C and 65.5°C respectively).

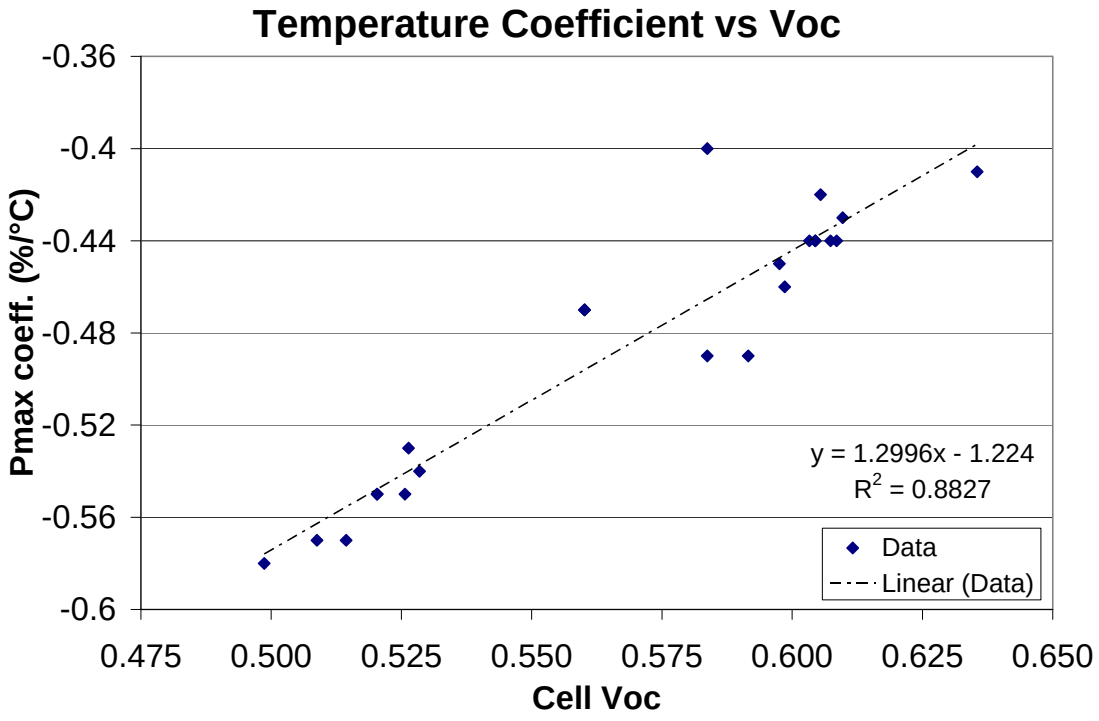

Fig. 2.19/ The measured thermal coefficient for output power as a function of open circuit cell voltage.

A comparison of the expected efficiency at temperatures corresponding to these two outdoor conditions is shown in table 2.4 for a low and high bandgap CIGS cell. The improvement in actual efficiency at elevated temperatures is significant, indicating the merit in this approach.

Table 2.4. Expected cell efficiencies with CIGS absorbers of large and small bandgaps at operating temperature. Cells are 13% efficient at standard conditions of 25°C.

	April (Tcell = 49.5°C)	**June (Tcell = 65.5°C)**	**Pmax (%/°C)**	**Tc**
Low Eg (Voc = 560 mV)	11.39	10.42	-0.496	
High Eg (Voc = 680 mV)	11.89	11.23	-0.340	
Absolute Efficiency Improvement	0.5%	0.81%		

Accordingly, a campaign to alter the Ga content and profile of the CIGS layer has been initiated at GSE. Cells with Voc's exceeding 700 mV have resulted recently from the bandgap engineering effort at GSE, without loss of overall efficiency. Thus, it seems feasible to reduce the temperature coefficient for power loss, attaining coefficients that are substantially below those typical for crystalline Si. The impact of the adjustments in the campaign to increase absorber bandgap is evident in the series of Voc measurements on sequential manufacturing lots, shown in fig. 2.20.

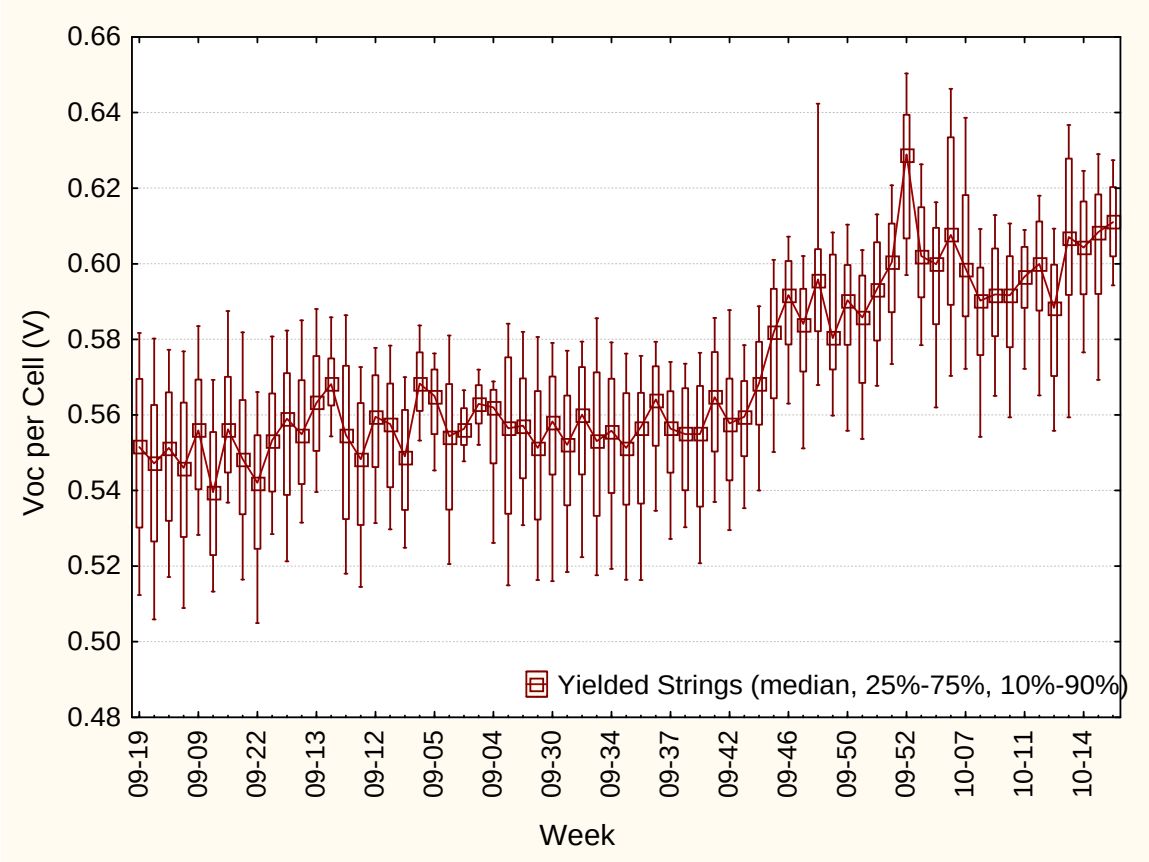

Fig. 2.20.Open circuit voltage (per cell) for "strings" on the production line at GSE, showing the initial impact of the campaign to increase the CIGS bandgap.

Process Development for Large Scale Production

Multiple challenges existed to raising efficiency and yield on the full scale production equipment, complicated by complexity of the processes and equipment. The major obstacles included:

1. Eliminating operational problems, deficiencies and design oversights in new equipment for all processes;
2. Establishing adequate process monitoring and metrics for all steps, with the ability to record, store, correlate and report them;

3. Assuring process reproducibility and control;
4. Optimizing process settings for an entire manufacturing sequence in which many process steps are interactive;
5. Training personnel, documenting critical procedures and establishing a qualified vendor network for critical parts and materials;
6. Transferring technology, results and procedures between factories in multiple countries to maintain equivalent capability;
7. Adaptation to new product introduction or major revision due to changing customer demand or technical capability.

Reproducibility and process control is crucial in meaningful process optimization during development and high yields in production. Process control is common to all seven of the factors mentioned above as obstacles to overcome in this progression. An example web, shown in Fig. 2.21, illustrates the consistency of key parameters achieved during this effort for a 1 km length. The setpoints are monitored in real time and used with intelligent closed-loop control to maintain the process. The displayed dependent variable (efficiency) represents the efficiency of entire 18-cell "strings" having 3780 cm^2 total area made from all locations downweb, at each of 3 locations crossweb. Independent variables are plotted to show the CIGS thickness and the composition rations of Cu/(In+Ga) and Ga/(In+Ga). The first 100 meters of the run is affected by a "start-up" effect – a phenomenon still under investigation that causes reduced efficiency despite proper setpoint values for all known process variables. Excepting this, there is very little variation over the entire course of the 1000 meter web in any of the parameters. All thin film deposition equipment typically runs unattended except where special intervention is necessary for special studies that require dynamic changes to parameter settings.

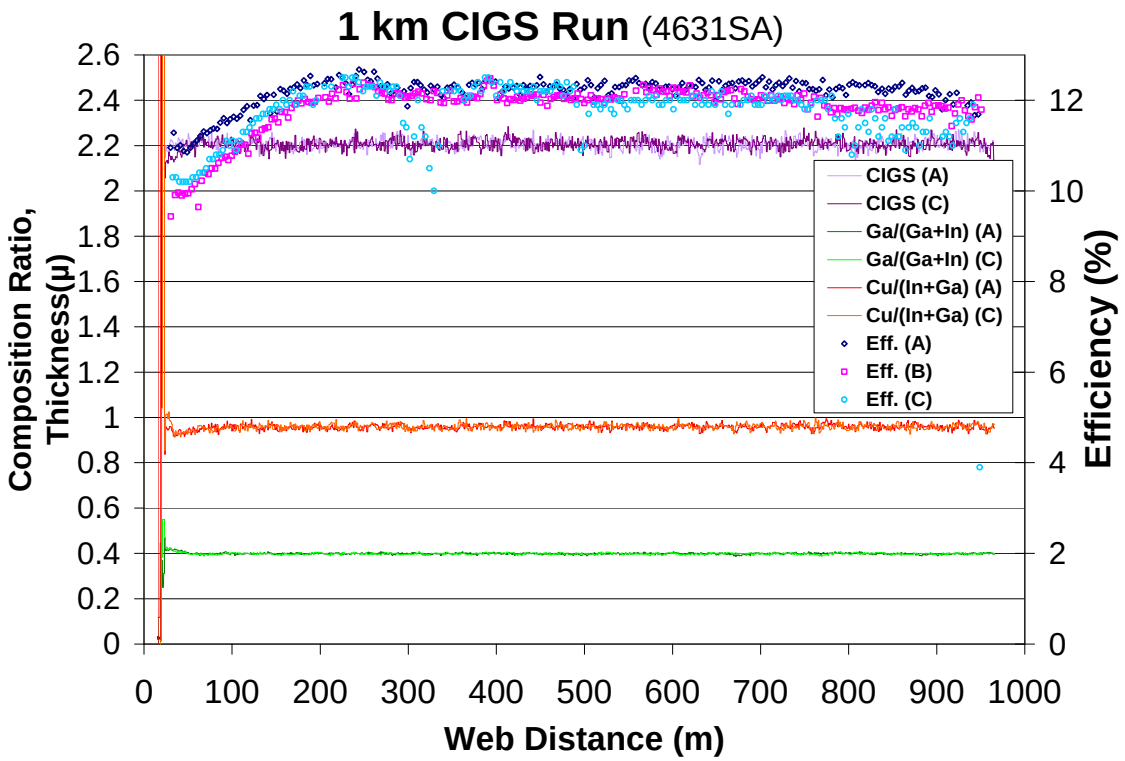

Fig. 2.21. ***Parameters of a 1 km web. Efficiency of strings made using 3 locations across the web, and independent parameters of CIGS thickness, Cu/(In+Ga) and Ga/(In+Ga) are shown at two crossweb locations down the entire web length. A "string" is 18 serially connected large area cells, each 210 cm^2 in area.***

Once control and reproducibility were achieved, many CIGS process tests were conducted to better understand the process space for maximized efficiency and minimized sensitivity. Some of the parameters explored were substrate temperature by zone, in-process Cu-rich excursion, final Cu/(Ga+In), Se delivery, and bandgap profile.

Task 3: Front Contact Cost Reduction (Objectives)

1. Develop a low-cost process for the transparent front contact TCO coating.
2. Improve deposition rate of the TCO process, while re-optimizing the process to maintain large-area cell efficiency above 12.5%.

Cost reduction in this step is important, as the TCO process was the single, most expensive thin film layer in the device stack upon initiation of this subcontract. A parallel approach using two paths has been taken for this task; a low-risk pursuit of marginal improvements using conventional sputtered methodology, and a high risk pursuit of a novel TCO deposition process potentially offering very large reductions in cost.

Novel TCO Deposition Process

The novel TCO deposition process is intended to avoid the requirement for sputtering targets, and those attendant costs with expensive target fabrication, limited target utilization and lifetime, maintenance and turnover labor thus yielding a cost improvement of an order of magnitude or more. An internal effort at GSE was initiated, as well as an effort carried out at a lower-tier subcontractor.

Toward that end in this period, a dedicated web coating chamber has been re-commissioned and made operational for development of the low cost TCO. The chamber has been fit with specialized mass flow control for two vapor-phase precursors, as well as up to 3 conventional gas feedstocks. Provisions were made for the addition of dopant in the dedicated chamber at GSE (called the "PE" chamber). Required ancillary provisions for a substrate heater and other monitoring instruments have also been installed in this roll-roll development chamber. A thermal decomposition reactor has been designed and fabricated to safely dispose of gas effluent expected of the process.

Exploratory experiments were completed depositing the low cost TCO on polyimide and stainless test webs. Sample TCO films (without any dopant) were also deposited on glass substrates for optical and electrical characterization. Some of the conditions yielded TCO films that were dense, uniform and well-adherent. The sheet resistivity of all films to date is high, as may be expected without any dopant.

Exploratory runs introducing varying levels of Al as a dopant to ZnO films were started. A first round of tests results show some reduction in sheet resistance, but still not approaching the low resistivity desired for TCO in films that are transparent and well adherent. Test depositions were primarily on glass witness slides.

A 2^{nd} round of statistically designed experiments have been completed in the "PE" chamber at GSE, showing some additional reduction in sheet resistivity while maintaining high transparency and adhesion, however a sheet resistivity in the desired range has still not been attained. Although reasonable growth rates have been attained in the "PE" chamber, the resistivity must be reduced by at least another factor of 4x, with reproducibility demonstrated.

Work at a lower-tier subcontractor to GSE with a specialized deposition method that is potentially low cost TCO was also started, referred to as the "ECS" method. The ECS method for deposition of ZnO has produced high resistivity films with good transparency and adhesion in a first round of experiments. Hall-effect mobility was low (1.2 cm^2/V-sec), and examination indicated the films typically had a large amorphous volume content. All films were done at low substrate temperatures and showed good uniformity of deposition in one dimension.

A further round of experiments with the ECS method gave reproducible results for the conductive ZnO, having improved carrier mobility in the range of 10-20 cm^2/V-sec, sheet resistivity of ~ 20 ohms/square and good optical transmission (shown in Fig. 3.1).

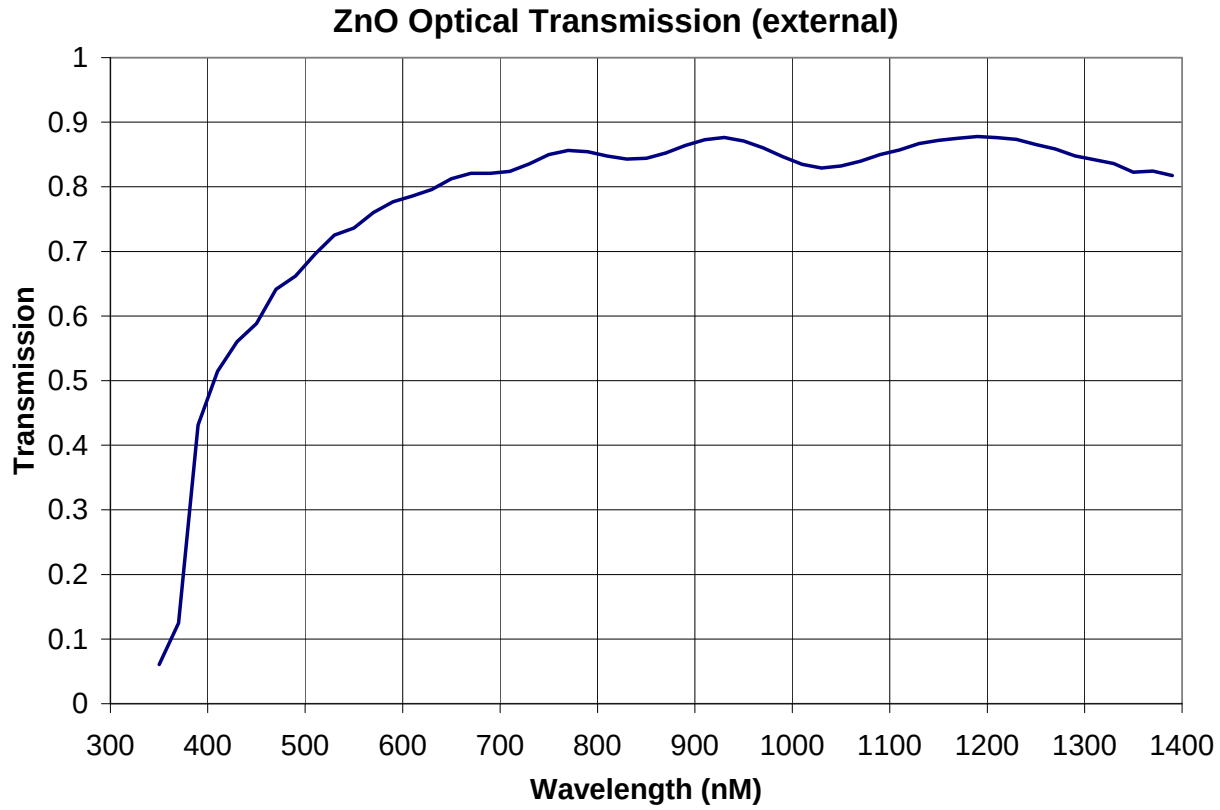

Fig. 3.1. The external optical transmission of a ZnO film on glass deposited using the "ECS" method at a lower-tier subcontractor to GSE. This film had a sheet resistivity of 22 ohms/square.

Materials properties have been evaluated and improved so that many key properties comparable to, or better than the standard TCO process used at GSE. The optical transmission of this alternate TCO process compares well with a typical process for ZnO having the same sheet resistivity (Fig. 3.2).

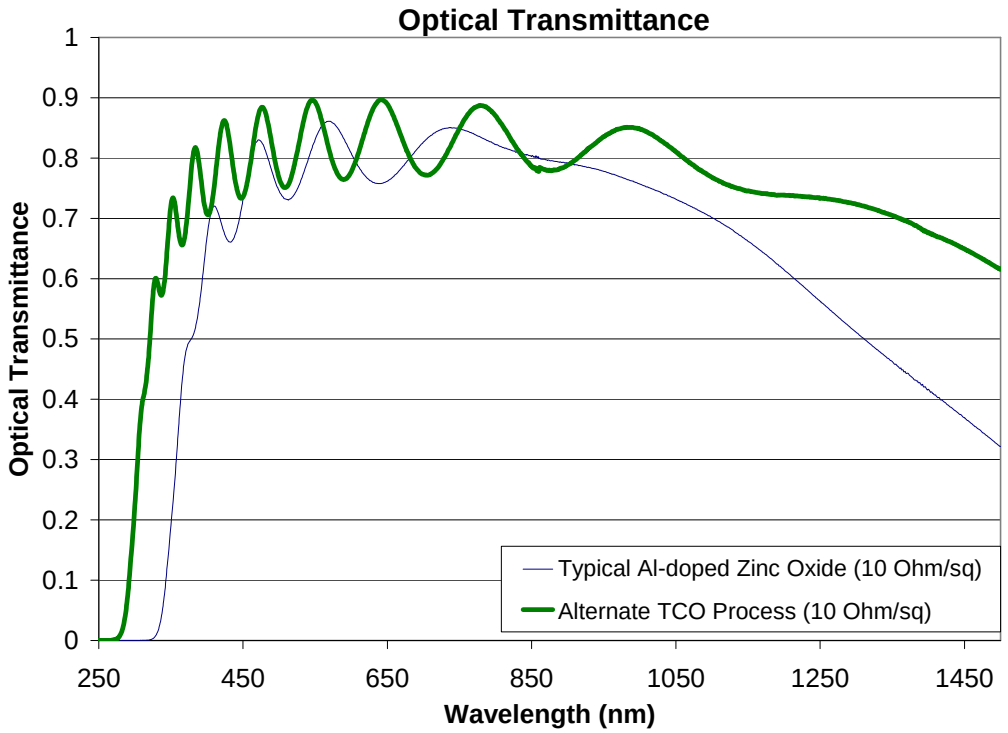

Fig. 3.2. The optical transmittance of TCO made using the alternate TCO process compared to Al-doped ZnO made using a typical process having the same sheet resistivity.

After materials studies confirmed the applicability of the alternate TCO process, several studies using standard CIGS PV were completed, encompassing designed experiments to optimize variables in a large parameter space. Device results for the most recent study are shown in Fig. 3.3 for the best 3 experimental conditions for TCO deposition using large area cells. In all cases the decrease in efficiency was accounted for in Voc and fill factor loss.

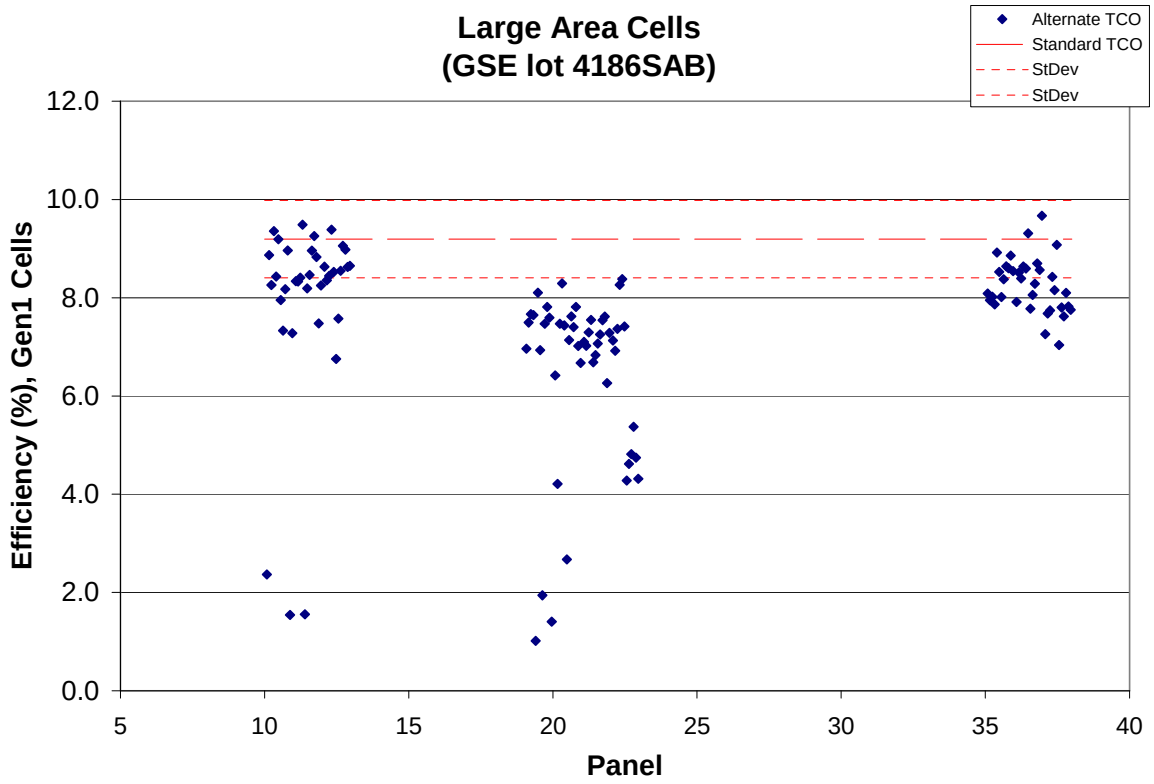

Fig. 3.3. Large area (68.8 cm^2) cell efficiency for GSE cells using the alternate TCO process. Each group of cells was processed at different conditions during TCO deposition. The standard TCO process is shown also for the same cell lot as dashed lines for the average cell efficiency ± 1 standard deviation.

Several factors remain to be proven regarding the ECS approach for TCO based on ZnO, including adequate deposition rate and controllability, stability of the ZnO properties, and compatibility of the ECS approach for ZnO deposition on actual device material. Although, under selected conditions, the alternate TCO process has produced large area cells that are comparable to the standard process, several aspects of the approach would require improvement, such as deposition rate, to make the process fully attractive.

Incremental Improvement of the Existing TCO Process: 'Gen1' Process

The incremental, low risk approach for TCO process improvement was implemented in two sequential efforts. Available remedies and improvements were applied to the 'Gen1' processes and equipments (designed around planar magnetrons). When the 'Gen2' equipment was designed and built, significant opportunities for process cost reduction were available, and acted on accordingly.

For the 'Gen1' equipment, lower cost ceramic targets were evaluated in first-cut experiments to reduce the cost of the TCO process. Arcing problems were pervasive, and thought to result from excessive clearance under the dark space shields coupled with excessive flake and debris generation. However, further experiments revealed that the actual cause of the variation in sputter voltage was intermittent plasma extinction due to a weak magnetic field at the target surface.

In spite of this problem, generation of production solar cells was attempted for measurement and reliability testing. Compared to the baseline top contact process, solar cells fabricated with the alternative TCO material had significantly lower yield, and maximum conversion efficiency was 8.6% compared to the maximum 11% for the control cells. The yield and quality of the solar cells generated was deemed insufficient for reliability evaluation. Further deposition experiments were planned using stronger cathode magnet arrays to stabilize the plasma.

Four new magnetic cathode arrays were installed to better evaluate the alternative TCO which had been evaluated previously. The improved magnetics resulted in a 640% improvement in voltage standard deviation. Once process control was achieved, coatings of the new TCO were applied to create solar cells for first reliability testing. The flexible modules produced were found to degrade more quickly than ITO control modules under accelerated testing (85˚C/85%RH). It is clear that the TCO deposited from these low cost targets must be modified to achieve better resistance to degradation in the "damp heat" (85˚C/85%RH) test.

The TCO thickness has been modified in the current production process and documented to give slightly better I-V performance concurrent with thinner TCO. Improved I-V performance arose due to a controlled shift of optical transmittance maxima to more desirable ranges of the solar spectrum, giving an Isc gain (shown in Fig. 3.4).

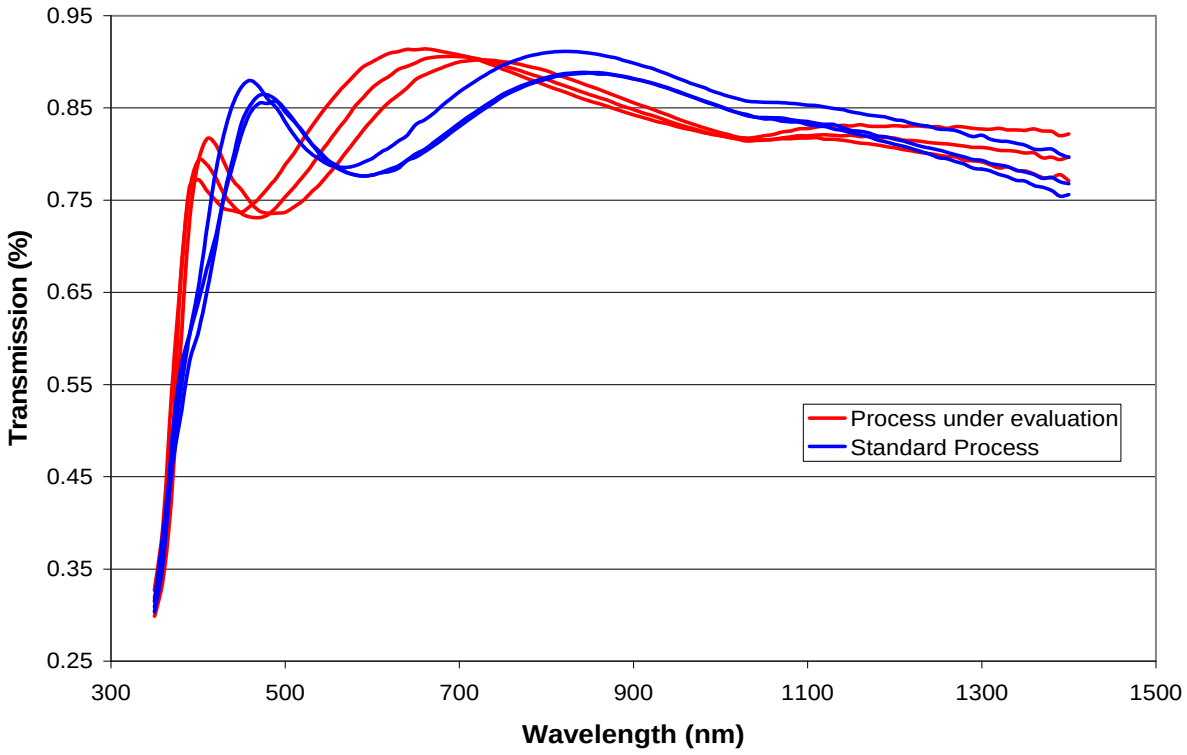

Fig. 3.4. A comparison of the optical transmission as a function of wavelength for the standard production TCO process and a new process under evaluation.

One goal in the 'Gen1' process was to improve bulk resistivity and thus enable a reduction in thickness, thus providing reduced cost and increased optical transmission at higher energy wavelengths. Process variables including the composition of the sputtering gas, pulsing frequency, and pressure were systematically varied in designed experiments. The resulting process enabled a 50% increase in line speed with an equivalent sheet resistance and integrated transmission. Optical measurements of coatings produced by the new process show reduced thickness shifting the transmission peak closer the 550nm. Large area cells were produced to demonstrate equivalence with the baseline process.

The modifications made to the gas composition and pressure results in 100% higher bulk conductivity. Moreover, the improved process also exhibits a better controlled sheet resistance over the course of a run (Figs. 3.5 a, b). Sheet resistance regulation of the new process is $\pm$ 32% absolute with a standard deviation of 14%.

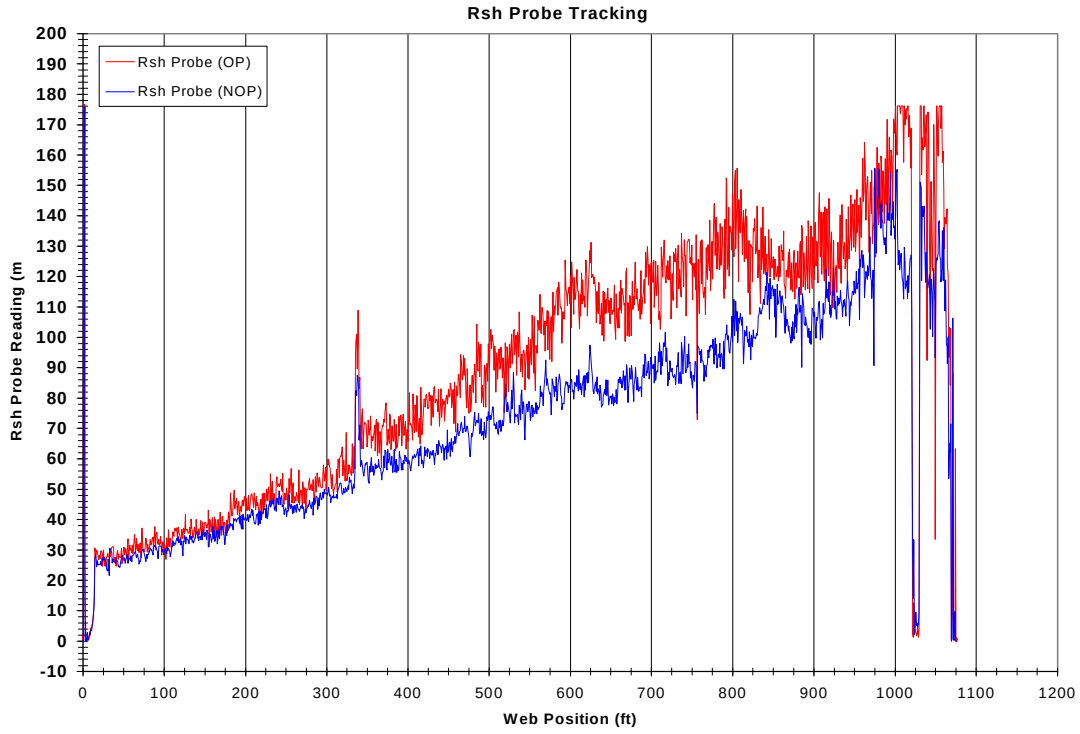

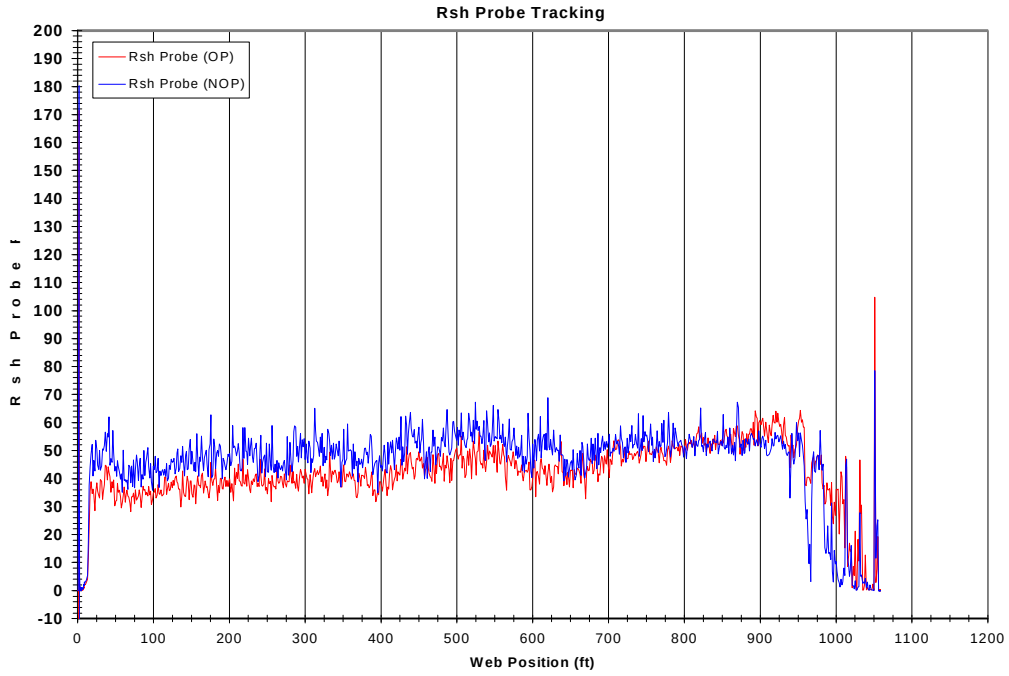

Figs. 3.5 a,b. A comparison of the sheet resistance behavior over the course of single runs for the previous process (upper plot) and the improved process (lower plot).

The data shown in Figs 3.5 a,b were taken in-situ, real-time for the TCO deposition using a 4-point probe having rolling contacts made of a soft, electrically conductive material (for example, an electrically conductive polymer). The rolling conductive contacts are mechanically independent as they are held against the moving web, thus are tolerant of irregularities.

The improved TCO process optimization nets GSE significant cost savings. Higher bulk conductivity enables the process to run 50% faster, enhancing throughput. Sputter power is reduced by 33%. Higher bulk conductivity also reduces the coating thickness required, increasing target material utilization.

'Gen2' (TCO) Process Scale-Up and Cost Improvement

The first TCO roll coater (TCO5) of the new design was delivered and installed at GSE during phase 2 of this subcontract. Subsequently, multiple identical tools were received, placed, facilitated and put into service at both the Tucson and Berlin facilities (Fig. 3.6). These TCO deposition tools were designed to be capable of well-controlled, uniform, high rate deposition using a dense array of rotary cathodes in a roll-to-roll approach.

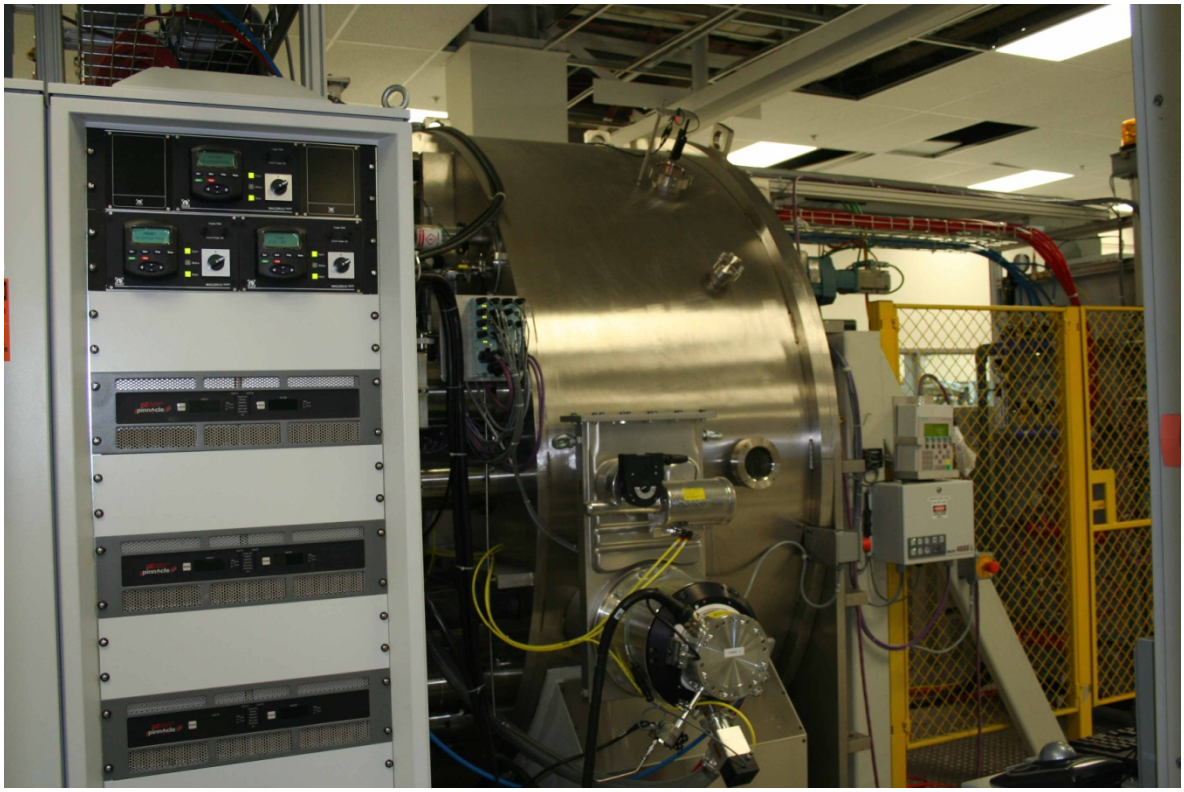

Fig. 3.6. The front contact (TCO) is deposited by pulsed DC magnetron sputtering. (Credit: Global Solar Energy)

Comprehensive plans were developed for bringing the tool on-line and integrating the process. The first major goal of the plan was to demonstrate coating capability and solar cell metrics comparable to those produced by the Gen1 TCO manufacturing equipment, applying a "hook and loop" approach where webs could be split and processed on a comparative basis in both "Gen1" and "Gen2" process equipment.

Subsequent to installation, campaigns have been initiated more fully utilize the equipment design to deposit at high rates, using high utilization sputtering targets, both factors being intended to reduce costs.

One example was the modification to attain more powerful magnet packs on the TCO targets to determine if faster deposition rates could be achieved. Faster deposition rates enable increased line speed and increased productivity for lower costs. With the new magnet packs, it was demonstrated that TCO cathode power could be decreased from 1400W to 1100W and maintain identical deposition rates. At an applied power of 1400W, cathodes with the new magnet packs allowed web speeds to be increased nearly 30%, with no loss in solar cell performance. All production systems were subsequently converted to the new packs.

These approaches are most often iterative, in that device performance is impacted by interactions so that changes in one parameter setting demand re-test of other parameter settings to garner full benefit. An example was a test conducted to evaluate the effect on cell performance of reduced power applied to deposit the insulating ZnO coating. For test conditions, the pulsed power to the

insulating layer targets was adjusted so that the power delivered to the targets was reduced by half, with no effect on the deposit thickness. Statistical analysis indicated no difference between the test samples and controls generated on the same lot (Table 3.1).

Table 3.1. Statistical comparison of IV parameters between reduced power i-ZnO and controls.

	Mean Test	Mean Control	t-value	df	p	Valid N Test	Valid N Control	Std.Dev. Test	Std.Dev. Control	F-ratio Variances	p Variances
Vmax	392.006	388.207	1.2626	166	0.208504	96	72	20.4722	17.6049	1.352254	0.182483
Imax	1786.153	1801.885	-0.83086	166	0.407244	96	72	137.0707	96.6604	2.010909	0.002303
Pmax	701.409	699.42	0.21189	166	0.832454	96	72	68.4228	46.9965	2.119682	0.001075
Voc	558.676	556.575	0.8884	166	0.375612	96	72	16.1677	13.717	1.389254	0.146521
Isc	2164.221	2172.617	-0.70681	166	0.480674	96	72	77.3668	74.6076	1.075333	0.752715
Fill Factor	57.914	57.838	0.11926	166	0.90521	96	72	4.677	3.1294	2.233678	0.000484
Efficiency	10.195	10.166	0.21193	166	0.832421	96	72	0.9945	0.6831	2.119691	0.001075
Rsh	853.78	976.034	-1.54358	166	0.124595	96	72	489.7579	531.4812	1.177641	0.454469
Rse	3.806	3.88	-1.32529	166	0.186898	96	72	0.3333	0.3827	1.31795	0.208519

Some effort during phase 2 was applied toward evaluations of the alternative sputtered TCO material. The alternative material is being evaluated as both an insulator against the buffer and as the front electrode. A variety of sputtering conditions were evaluated for their effects on solar cell performance. A wide distribution of cell efficiencies resulted from all deposition conditions evaluated, although maximum efficiencies were comparable to the standard production process. No conclusions could be reached due to the diminished yield. The higher performing solar cells were fabricated into strings for reliability testing of flexible and glass laminated modules outdoors and in damp heat.

Overall, the cost reduction effort for TCO has been successful, mostly due to the improved design enabled by the transition to the ‘Gen2’ equipment. The use of rotary cathodes in a compact format allow a higher web coating rate in compact equipment (low capital cost) and much better materials utilization. The planar magnetron targets used in the ‘Gen1’ equipment often were expended after only 20% - 30% of the target material was used, due to the ‘racetrack’ wear pattern. The rotary cathodes implemented in the ‘Gen2’ equipment can approach 90% use of the target material before replacement. Initially the sputtering targets for the rotary cathodes were very expensive, but continual work with vendors has allowed a continual reduction in target costs.

Task 4: Back Contact Cost Reduction and Efficiency Improvement (Objectives)

1. Evaluate substrate properties and analyze resulting impacts on device performance.
2. Quantify impacts of reduced Mo thickness and correlate to device performance.
3. Examine low-cost alternate back contact materials for partial substitution of Mo and compare device performance and other properties against the established baseline.
4. Demonstrate increased device efficiencies and reduced process costs through material savings and increased process speeds.
5. Integrate alternate sodium delivery to maximize adhesion and efficiency at the higher CIGS web processing rate.

Back Contact Process Improvements

Designed experiments using large-area cells indicated that cell performance is unchanged despite a reduction in the thickness of the back contact interface material of up to 50%, presenting an opportunity for reducing materials costs and process time. However, thickness changes in the molybdenum layer itself from the standard value resulted in a loss in cell performance.

In subsequent tests, a 12% reduction in Mo thickness on string performance was evaluated using a test web prepared with control sections at the web ends and two interior sections with Mo thicknesses 94% and 88% of the controls. Slight reductions in string efficiency were observed for sections with thin Mo, but the differences were not statistically significant. Further tests were run to understand the process sensitivity to Mo thickness, and the potential for thickness (and cost) reduction. In general, the results indicated that Mo thickness reduction below a certain value caused a loss in efficiency that could not be avoided by other process changes.

In another series of experiments the effects of deposition parameters on the morphology of the Mo layer and the subsequent effects on cell performance were evaluated. Parameters included were temperature, pressure, and gas partial pressures. We evaluated morphology by SEM, structure by XRD, adhesion of the Mo/CIGS interface by pull testing and cell performance. The morphology of the deposited Moly film was confirmed as columnar growth. XRD analysis revealed mixed orientations on the stainless steel substrate. We observed an impact on cell performance at distinct points in the Mo process study, and this improved understanding led to changes in processing parameters that yielded better process control and homogeneity over the length of the web.

Prior to starting the back contact deposition, the chamber is run through a “conditioning” procedure. The conditioning procedure was changed in systematic experiments to improve deposition consistency. The results indicated no benefit to actual material consistency or quality, however the process reliability was improved due to reduced arcing over the course of production runs.

Modifications to the start-up sequence and pump-down requirements were also investigated to increase throughput in the Mo sputter process. Several modifications were successfully implemented that reduced the time required between depositions for preparation and pumpdown.

Deterioration of roller surfaces as well as flakes of deposited molybdenum shed from zone shielding were observed to introduce defects on the web. Modifications were made to the deposition shields and process in the production coaters to minimize shedding. Other web defects caused by uneven tension of the metal foil during deposition were also identified. Interactions between web tension, deposition temperature, roller alignment in the chamber and shape of the foil (camber) were investigated as a possible cause for the tension-related defects.

Alternate Substrate Vendors and Materials

Testing of the stainless steel foil used for substrate material supplied by alternate vendors to GSE has started. As the pricing and quality of the incoming substrate material vary significantly, this effort has fairly large potential impact on total cost. Sample steel coils were received from 3 alternate vendors, and orders placed for sample coils from another two during this period. Substrate cleaning methods are also important apart from surface and mechanical properties or

chemical composition, however, and must be evaluated concurrently with the material from other manufacturers. Evaluation of the incoming substrate material from different vendors is ongoing.

Joining webs seamlessly is an important capability for direct comparison of different substrate material in a roll-to-roll process. A method was established for joining web sections at GSE that enables more reliable and efficient testing and designed experiments. Different sections of various substrates can be processed under identical conditions. Alternatively a web can be split at any process and with each section undergoing separate treatment. After that step, the web can be joined together to complete identical processing for all other process steps.

The experience in comparative evaluation of substrate from different vendors identified a need for a standardized battery of tests for incoming metal foil. A survey of applicable techniques and equipment to characterize the important properties of the incoming substrate material has been assembled. As a result, GSE has identified optical surface profilometry as a primary measurement capable of giving quantitative information about important properties of incoming metal foil. Several optical profilers were evaluated, with one selected for purchase.

New vendors were also tested and successfully qualified for sputtering targets of Mo and other required back contact materials, giving multiple redundancies in vendors and a cost savings in some cases.

Materials Substitution and Reduced Cost

Substantial opportunity to reduce total cost often exists in the form of material substitution, using either less expensive grades of a constituent from a current supplier, or equivalent materials that are available at better prices from new vendors. A careful evaluation of current spec requirements was performed. Furthermore, this opportunity is driven by a growing diversity of global sources for some materials, new and better techniques for meeting materials requirements, and a growing recognition among materials suppliers of the importance of the PV market and a desire to enter that market.

In one case, an alternative grade of stainless steel became available from our primary supplier. Analysis revealed that some components of the alloy were found in higher concentration than in our baseline stainless steel. The advantage of the alternate stainless foil was less difficulty in processing into roll form, equating to lower price and better characteristics in some areas. However, the performance of production lots fabricated on the new alloy was significantly lower than that of the controls fabricated on the standard stainless steel. Several of the new alloy's characteristics were quantified to determine assignable cause for the reduced performance.

In another instance two new suppliers of stainless steel and another supplier previously investigated were evaluated. The supplier previously investigated (and found unsuitable) was re-considered because new cleaning techniques had been applied to their product. Upon re-evaluation of the latter by processing several of the new coils through the production line, the product was again found to lead to inadequate performance. However, one of the new suppliers was found to provide performance comparable to the qualified supplier. Additional, more extensive qualification tests are planned for the new potential supplier.

Besides the substrate itself, the materials used for the back contact coating also represent a significant expense, and thus an opportunity to reduce costs.[6] Alternative suppliers of molybdenum were evaluated to better understand the potential effects of common impurities on the performance and yield of the resulting PV product. Four lots of material from each supplier were processed through standard production. When compared to controls, no statistically significant difference in lot performance was seen between any of the alternative suppliers for different target types.

Preliminary studies like these are often used as a basis to evaluate still other suppliers and materials preparation methods, where potential cost savings warrant, as illustrated by the evaluations below that were made during phase 2.

- Sputtering cathodes from two suppliers were received and evaluated. The simpler, more robust and serviceable of the two cathodes was down-selected for utilization in the new Gen2 sputtering systems.
- Sputtering targets compatible with the Gen2 molybdenum sputtering chambers were procured from multiple suppliers. The molybdenum targets, prepared by different techniques, were evaluated in one of the Gen1 sputtering chambers with a fixture to accommodate the new target geometry. The targets were installed on a Gen2 cathode and evaluated for compatibility with the cathode, coating deposition rates on a moving web, and the condition of the target surface after extended sputtering periods. From these results the new targets were down-selected from multiple suppliers.
- A less costly technique for molybdenum target fabrication was evaluated in the Gen1 equipment. Deposition rates under standard conditions were evaluated first, with no significant differences in deposition rates observed. However, test lots made using the alternative targets for production line solar cells showed significantly lower performance than cells using the standard molybdenum targets. The performance difference was linked to specific impurities not found in the standard targets. Since then an alternate target fabrication method that allows for cost reductions has been tested and has been qualified for production.

Significant progress has been made using re-selection and substitution of materials and suppliers for the back contact. Many, although not all, of the trials yielded positive results and were down-selected for production use.

"Gen2" Back Contact Equipment Installation and Characterization

As previously mentioned, the increase in deposition rate and length purposely designed into the "Gen2" deposition tools for all thin film coating steps is an integral part of the cost reduction plan at GSE. Installation of the first roll coater for the back contact (Moly 5) was completed in early January of Phase2. Similar to the deposition tool for the front contact, the first major goal was to demonstrate coating and solar cell metrics comparable to those produced by the Gen1 back contact manufacturing equipment, applying the "hook and loop" approach. The capability of Moly 5 to produce individual solar cells with efficiency greater than 10% was demonstrated within a few depositions.

However, the first test webs coated in Moly 5 had significant mechanical defects in the form of scuffs, scratches, and impressions. These defects were correlated with shunted solar cells. Modifications were made to shielding in the web path to guarantee sufficient clearance. The rollers and other components controlling the web motion were aligned to tighter tolerances. Consequently, the mechanical defect density was dramatically reduced. However, defects continued to be present at a reduced level down the web length.

Non-uniform web tension may be responsible for some physical defects. A number of tests were conducted to explore parameters that could provide more uniform tension, including web temperature and coating stress. The applied sputter power represents a considerable amount of the total energy contributing to web heating. High line speeds and therefore high sputter power are required for an economical manufacturing process. On the other hand, control of the substrate temperature and its effects on the structure and shape of the foil are important for good quality of the material. This line of investigation is continues with a goal of complete elimination of the remaining defects.

At GSE, the Mo coating thickness is typically characterized by XRF. Along the majority of a typical web, the Mo thickness uniformity is +/- 3%, with the thinnest coating occurring in the web center (Fig. 4.1). Thinner Mo coating is frequently observed in the first 100m of deposition, with causes under investigation.

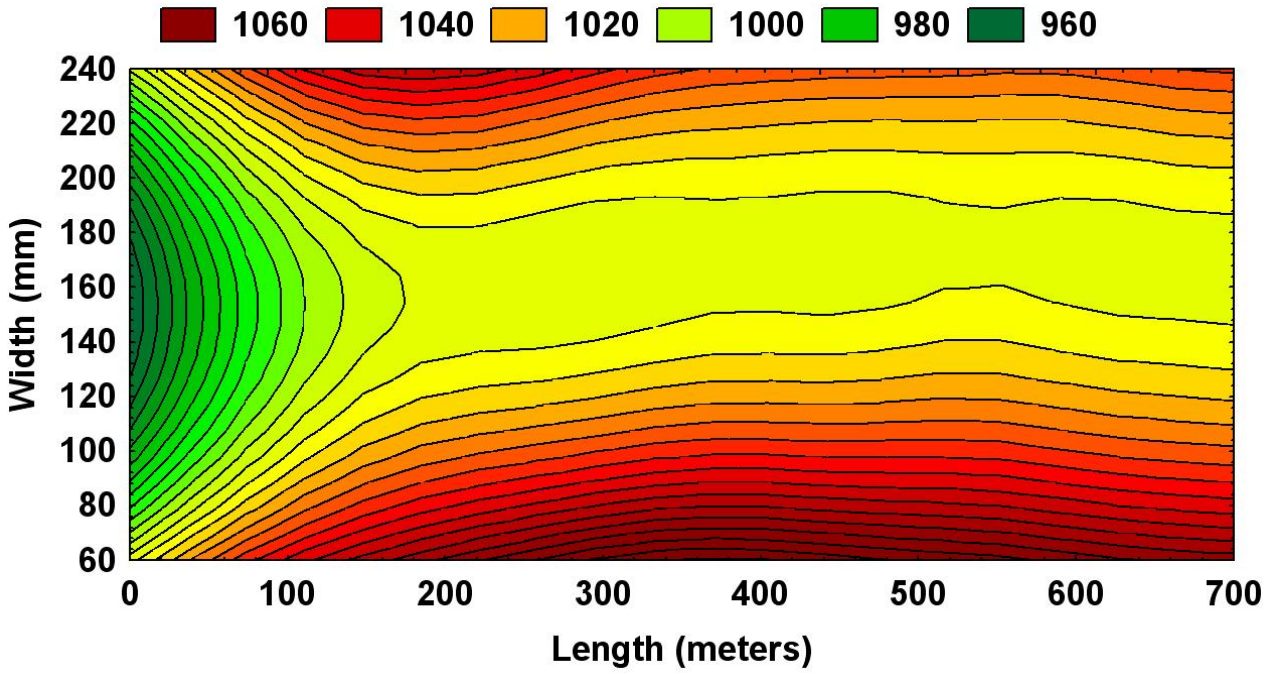

Fig. 4.1. A contour plot of Mo thickness (a.u.) down and across the web as measured by XRF (distance weighted least squares fit

One aspect affecting reliability is the thickness and conditions used to deposit molybdenum layers on the stainless steel substrate, as eventually the large area cells are serially connected in the module fabrication step and electrical contacts are established to the molybdenum-coated stainless.

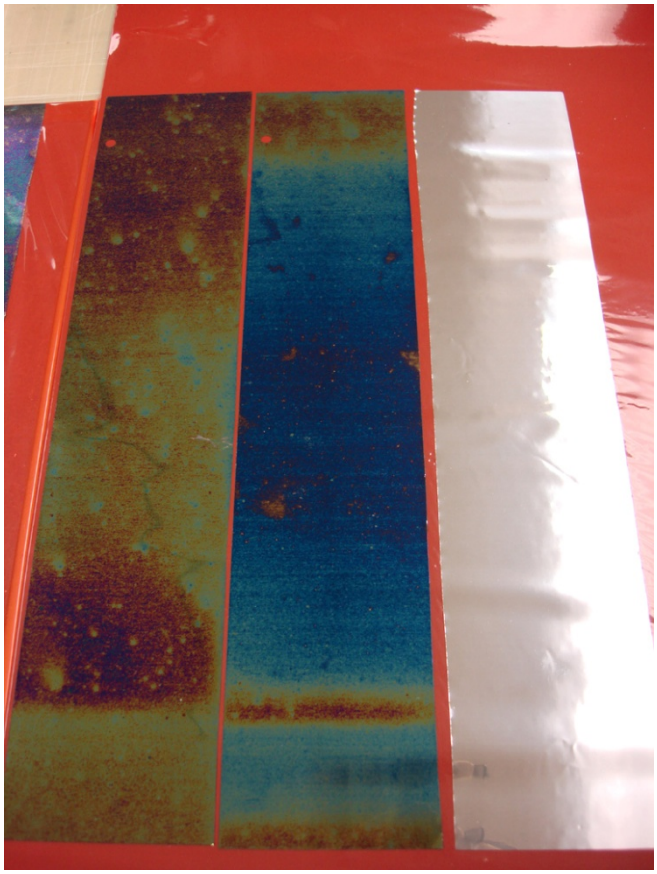

Fig. 4.2. Three coupon samples of substrate material with various coatings after 24 hours exposure to damp heat (85°C/85% RH), visually showing a differing response. (Credit: Global Solar Energy)

Reliable electrical contacts to the molybdenum-coated substrate are required, yet the molybdenum is easily oxidized in the presence of moisture and oxygen. Because damp heat testing is an important part of the qualification regimen for the PV product, the impact of damp heat exposure on the reliability of the contacts to the substrate was investigated. Oxidation of the surface layers caused by damp heat (85°C/85% RH) exposure is clearly visible (fig. 4.2). Sets of tests were run comparing the mechanical and electrical characteristics of contacts made to substrate material as a function of the thickness and conditions used for the molybdenum deposition. One example of the electrical response after damp heat exposure of contacts made to substrates having molybdenum deposited with different characteristics is shown in fig. 4.3. In this test series resistance was measured in a standardized structure using ribbon contacts to the PV substrate, simulating actual module construction. Variation between different groups is evident, indicating that the change in electrical resistance at module interconnections during moisture exposure is affected by the characteristics of the molybdenum deposition for the PV substrate.

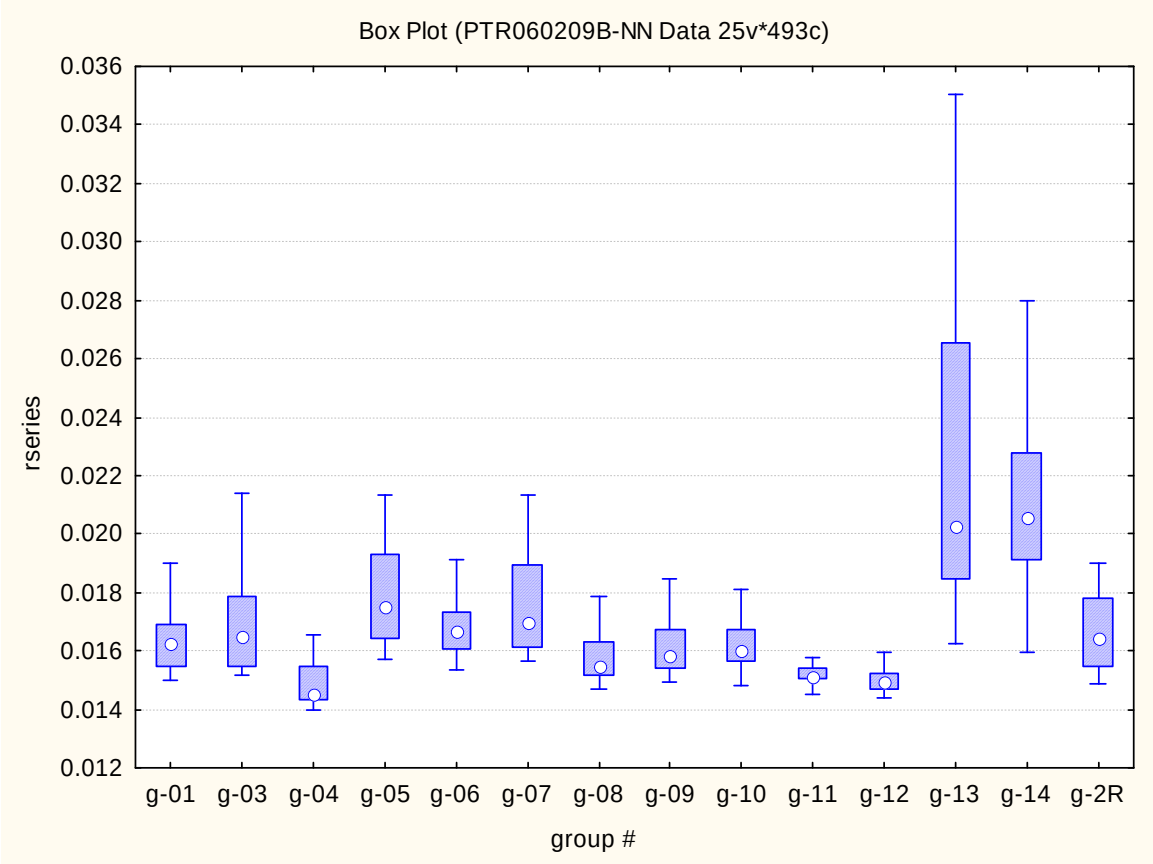

Fig. 4.3. The series resistance of ribbon contacts made to the molybdenum coated PV substrate after only 16 hours of damp heat (85°C/85% RH) exposure, indicating a dependence of magnitude and variability on the test group. Each test group represented different deposition conditions for the molybdenum overlayer.

Mechanical properties were also tested (fig. 4.4), looking at the impact of various molybdenum deposition thicknesses and conditions on ribbon bond strength.

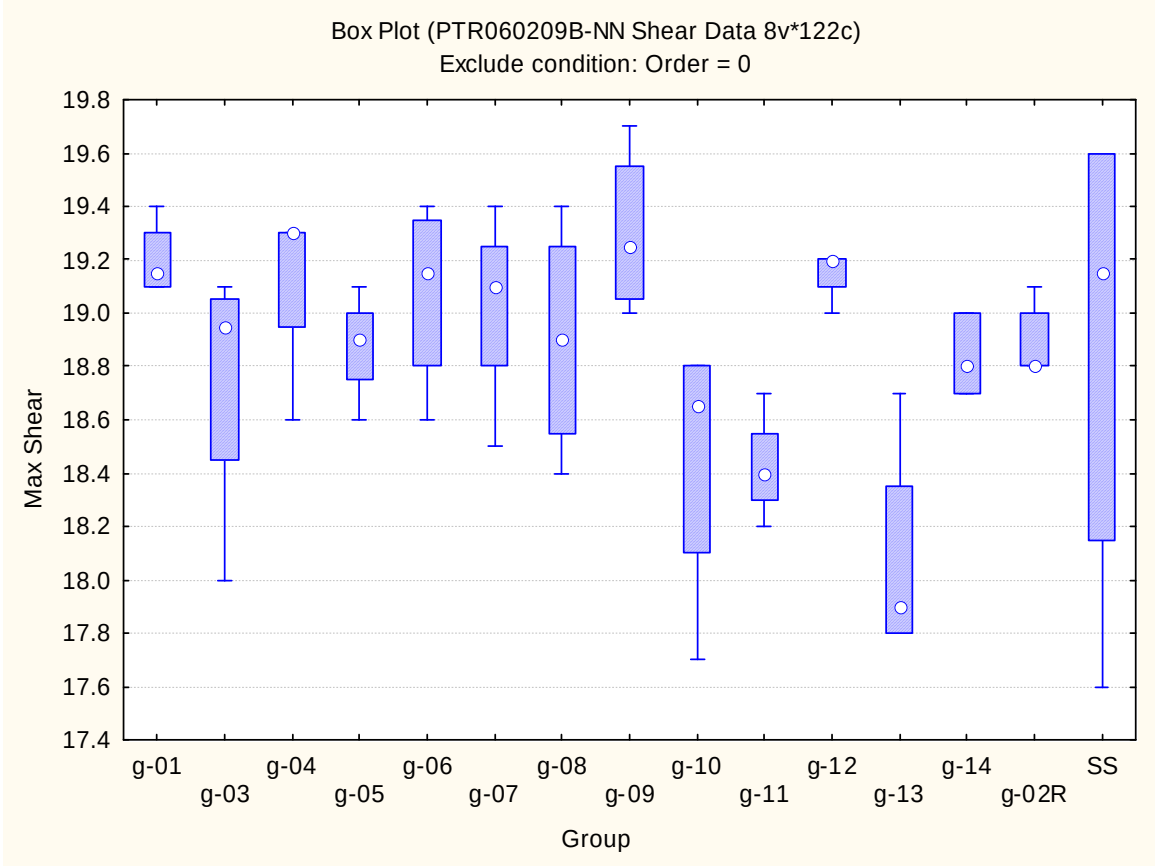

Fig. 4.4. The mechanical strength of ribbon contacts made to the molybdenum coated PV substrate after only 8 hours of damp heat (85°C/85% RH) exposure. The test groups correspond to those in Fig. 4.3., representing different deposition conditions for the molybdenum overlayer.

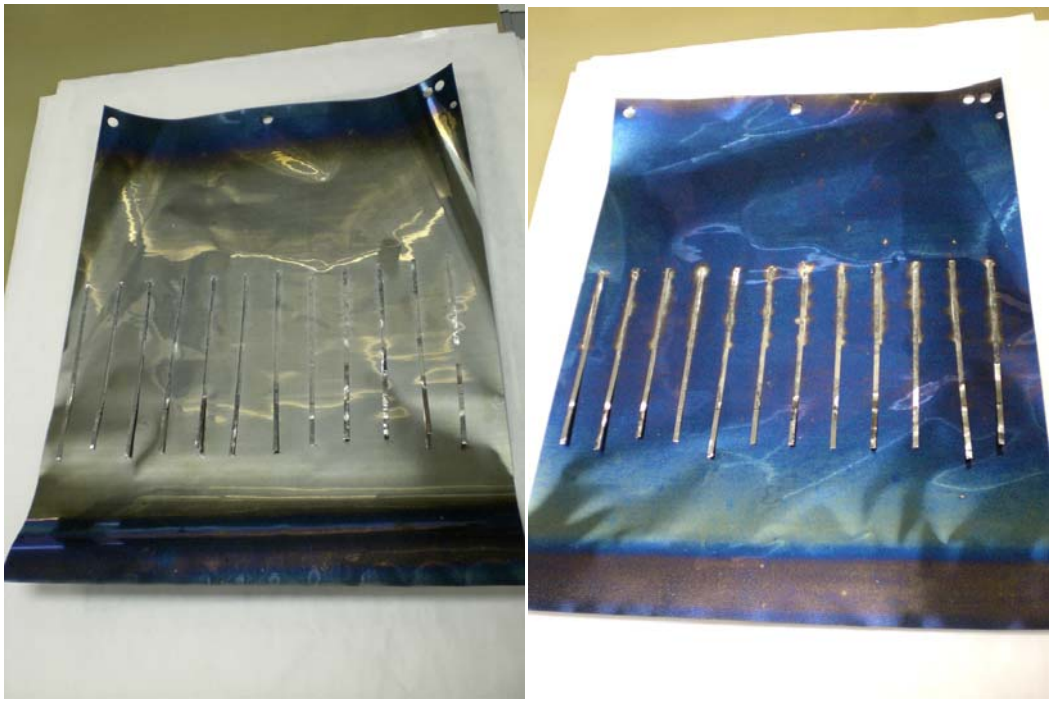

Fig. 4.5. Visual appearance of the ribbon contact test structures made to the molybdenum coated PV substrate was observed to vary significantly after damp heat (85°C/85% RH) treatment depending on Mo deposition conditions. This figure shows samples from groups 4 and 5 after 8 hours of damp heat exposure. (Credit: Global Solar Energy)

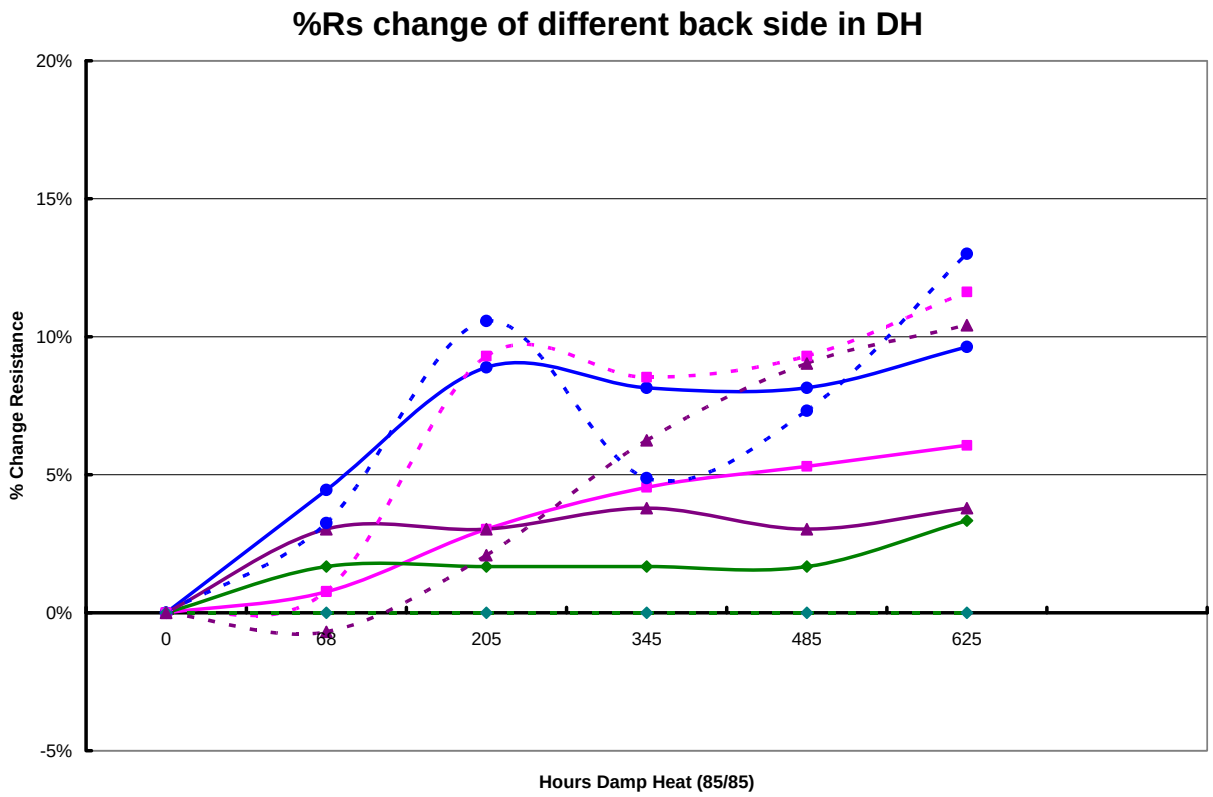

Fig. 4.6. ***A plot of the change in series resistance vs damp heat exposure time for ribbon connections made under different conditions to the backside contact. All conditions including the GSE standard process show Resistance increases of < 15% after 600 hrs in DH.***

Although work to understand the behavior and role in failure modes of the back contact continue, we have successfully reduced the increase of the series resistance from the back contact to less than ~15% (fig. 4.6). Recent tests show stable series resistance of a number of interconnects in unencapsulated cells out to 800 hrs in damp heat conditions.

References

[1] J.S. Britt, S. Wiedeman, U. Schoop, and D. Verebelyi, “High-Volume Manufacturing of Flexible and Lightweight CIGS Solar Cells,” 33rd IEEE PVSC, 2008, pp. 1670.

[2] M.E. Beck, S. Wiedeman, R. Huntington, J. VanAlsburg, E. Kanto, R. Butcher, and J.S. Britt, “Advancements in Flexible CIGS Module Manufacturing,” 31st IEEE PVSC, 2005, pp. 211-214.

[3] J.S. Britt, E. Kanto, S. Lundberg, M. E. Beck, “CIGS Device Stability on Flexible Substrates,” 4th World Conference on Photovoltaic Energy Conversion (IEEE), 2006, pp. 352-355

[4] W.N. Shafarman, R. Klenk, and B.E. McCandless, "Device and Material Characterization of Cu(In,Ga)Se2 Solar Cells with Increasing Bandgap," *J. Appl. Phys*. **79**, 1996, pp. 7324.

[5] D.L. King, J.A. Kratochviland, and W.E. Boyson, “Temperature Coefficients for PV Modules and Arrays:Measurement Methods, Difficulties, and Results,” 26th IEEE PVSC, 1997, pp. 1183-1186.

[6] J.S. Britt, R. Huntington, J. VanAlsburg, S. Wiedeman, and M. E. Beck, “Cost Improvement for Flexible CIGS-Based Product,” 4th World Conference on Photovoltaic Energy Conversion (IEEE), 2006, pp. 388-391.